



This is an authorized facsimile  
printed by microfilm/xerography on acid-free paper  
in 1984 by  
UNIVERSITY MICROFILMS INTERNATIONAL  
Ann Arbor, Michigan, U.S.A.

3267



Bacigalupo, Juan

A STUDY OF THE LIGHT-ACTIVATED CHANNELS IN LIMULUS VENTRAL  
PHOTORECEPTORS

Brandeis University

Ph.D. 1984

University  
Microfilms  
International

300 N. Zeeb Road, Ann Arbor, MI 48106



## INFORMATION TO USERS

This reproduction was made from a copy of a document sent to us for microfilming. While the most advanced technology has been used to photograph and reproduce this document, the quality of the reproduction is heavily dependent upon the quality of the material submitted.

The following explanation of techniques is provided to help clarify markings or notations which may appear on this reproduction.

1. The sign or "target" for pages apparently lacking from the document photographed is "Missing Page(s)". If it was possible to obtain the missing page(s) or section, they are spliced into the film along with adjacent pages. This may have necessitated cutting through an image and duplicating adjacent pages to assure complete continuity.
2. When an image on the film is obliterated with a round black mark, it is an indication of either blurred copy because of movement during exposure, duplicate copy, or copyrighted materials that should not have been filmed. For blurred pages, a good image of the page can be found in the adjacent frame. If copyrighted materials were deleted, a target note will appear listing the pages in the adjacent frame.
3. When a map, drawing or chart, etc., is part of the material being photographed, a definite method of "sectioning" the material has been followed. It is customary to begin filming at the upper left hand corner of a large sheet and to continue from left to right in equal sections with small overlaps. If necessary, sectioning is continued again—beginning below the first row and continuing on until complete.
4. For illustrations that cannot be satisfactorily reproduced by xerographic means, photographic prints can be purchased at additional cost and inserted into your xerographic copy. These prints are available upon request from the Dissertations Customer Services Department.
5. Some pages in any document may have indistinct print. In all cases the best available copy has been filmed.

University  
Microfilms  
International  
300 N. Zeeb Road  
Ann Arbor, MI 48106

MEMORANDUM

1. The purpose of this memorandum is to provide information regarding the proposed changes to the existing contract between the Government and the contractor.

2. The proposed changes are as follows:

3. The proposed changes are as follows:

4. The proposed changes are as follows:

5. The proposed changes are as follows:

6. The proposed changes are as follows:

7. The proposed changes are as follows:

8. The proposed changes are as follows:

PLEASE NOTE:

In all cases this material has been filmed in the best possible way from the available copy. Problems encountered with this document have been identified here with a check mark ✓.

1. Glossy photographs or pages ✓
2. Colored illustrations, paper or print \_\_\_\_\_
3. Photographs with dark background ✓
4. Illustrations are poor copy ✓
5. Pages with black marks, not original copy \_\_\_\_\_
6. Print shows through as there is text on both sides of page \_\_\_\_\_
7. Indistinct, broken or small print on several pages ✓
8. Print exceeds margin requirements \_\_\_\_\_
9. Tightly bound copy with print lost in spine \_\_\_\_\_
10. Computer printout pages with indistinct print \_\_\_\_\_
11. Page(s) \_\_\_\_\_ lacking when material received, and not available from school or author.
12. Page(s) \_\_\_\_\_ seem to be missing in numbering only as text follows.
13. Two pages numbered \_\_\_\_\_. Text follows.
14. Curling and wrinkled pages \_\_\_\_\_
15. Other \_\_\_\_\_

University  
Microfilms  
International





A STUDY OF THE LIGHT-ACTIVATED CHANNELS IN  
LIMULUS VENTRAL PHOTORECEPTORS

A DISSERTATION

Presented to  
The Faculty of the Graduate School of Arts and Sciences  
Brandeis University  
Department of Biology

In Partial Fulfillment  
of the Requirements of the Degree  
Doctor in Philosophy

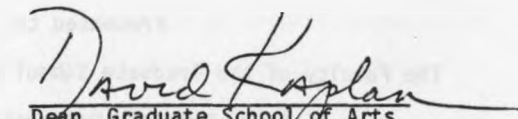
by

Juan Bacigalupo

October 1983

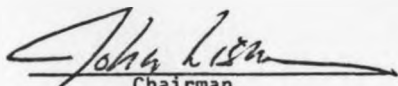
This dissertation, directed and approved by the candidate's Committee, has been accepted and approved by the Graduate Faculty of Brandeis University in partial fulfillment of the requirements for the degree of

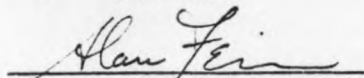
DOCTOR OF PHILOSOPHY

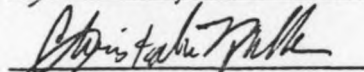
  
Dean, Graduate School of Arts  
and Sciences

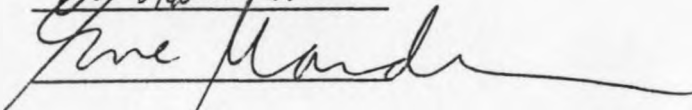
FEB 1 1984

Dissertation Committee

  
Chairman







### ACKNOWLEDGEMENTS

I am indebted to my advisor, John Lisman, for giving me the opportunity to work in the captivating field of photoreceptors, for the many things that I learned from him during the years I spent in his laboratory and for his generosity. I am also indebted to the members of the Biology Department for being so kind and helpful to me during my stay in this Department. I wish to especially thank Eve Marder, Andrew Szent Gyorgyi and Jeff Hall, from whom I received much important advice that became relevant in different aspects of my scientific education. From Chris Miller and Irwin Levitan I received invaluable help and encouragement during this work.

I would like to express my deep gratitude to Dr. Mario Luxoro, from the Faculty of Sciences on the University of Chile, for his very important role in my scientific education. I also thank Drs. Francisco Bezanilla, Osvaldo Alvarez, Humberto Maturana and other professors from the same school, from whom I also received invaluable help during my early years in science.

I also thank Wolfgang Hanke for long discussions about my data.

To David Stokes I thank his important help on experiments included in Chapter II.

To Cecilia Vergara I thank for the most I have.

I also wish to thank my fellows in the laboratory, especially Kevin D. Chinn, for their friendship and invaluable discussions.

I also like to thank my friends of the "chilean maffia" for giving me a constant moral support during my years at Brandeis.

I am also very indebted to Dave Eaton, from the machine shop, whose help in building my set-up was essential to the work of this thesis.

... and to many others.

During the years of my graduate studies I was generously supported by a fellowship from Brandeis University.

Part of this work (Chapter II) was done in collaboration with Jeff Stern and Kevin Chinn.

To my mother

## TABLE OF CONTENTS

Acknowledgements.....	1
Table of Contents.....	iii
List of Illustrations.....	iv
Chapter I: Introduction to the Thesis.....	1
Chapter II: Distinct Lobes of <u>Limulus</u> Ventral Photoreceptors.	
Functional and Anatomical Properties of Lobes Revealed by	
Removal of Glial Cells.....	7
Summary.....	8
Methods.....	9
Results.....	11
A. Denuding the Ventral Photoreceptor.....	11
B. Scanning Electron Microscopy of Ventral Photoreceptors.....	15
C. Sensitivity of the R-lobe and the A-lobe to Light.....	18
D. Light Adaptation is Initiated at the R-lobe.....	20
Discussion.....	22
Chapter III: Properties of Light-activated Channels in <u>Limulus</u>	
Ventral Photoreceptors.....	25
Summary.....	26
Methods.....	27
The Preparation.....	27
The Experimental Apparatus.....	29
Patch-clamp Recording.....	30
EGTA injections.....	30
Results.....	33
A. Activation of Single-channel Currents During Illumination....	33
B. Intensity- and Time-dependence of the Single-channel	
Activation.....	37
C. Effect of Light Adaptation on the Single-channel Response....	40
D. $\text{Ca}^{2+}$ Does Not Mediate the Activation of the Channel by Light.	41
E. Properties of the Individual Light-activated Channels.....	45
Discussion.....	53
Previous Evidence for Channels in Photoreceptors.....	53
Evidence for the Light-activation of the Channels.....	54
Similarities between the Single-channels and the Macroscopic	
Light-activated Conductance.....	54
Differences between the Single-channels and the Macroscopic	
Light-activated Conductance.....	57
Possible Effect of $\text{Ca}^{2+}$ on the Light-activated Channel.....	58
Comparison of the Properties of the Light-activated Channel and	
the Acetylcholine Channel.....	59
Implications of the Single-channel Basis for the Light-activated	
Conductance with Regard to Transduction.....	61
References.....	63

## LIST OF ILLUSTRATIONS

II-1	: Ventral Photoreceptors Under the Light Microscope Before and After Removal of glial cells.....	12
II-2	: Ventral Photoreceptor Under the Scanning Electron Microscope Before Removal of Glial Cells.....	14
II-3	: Denuded Photoreceptor Under the Scanning Electron Microscope..	16
II-4	: Scanning Electronmicrograph of Photoreceptor having two R-lobes and one A-lobe.....	17
II-5	: Differential Sensitivity to Light of the A-lobe and R-lobe....	19
II-6	: Effect of Position of Adapting Spot on Subsequent Sensitivity to Light.....	21
III-1	: Diagram of the Patch-clamp Circuit.....	31
III-2	: Single-channel Response to Light.....	34
III-3	: Light-induced Depolarization Does Not Mediate Channel Activity.....	36
III-4	: Single-channel Responses to Light Stimuli of Increasing Intensities.....	39
III-5	: Effect of an Adapting Light on the Single-channel Response....	42
III-6	: Effect of EGTA on Channel Activation.....	44
III-7	: Current-Voltage Relationship for the Single Light-activated Channel Currents.....	46
III-8	: Semilog Plot of the Distribution of Open Times.....	48
III-9	: Voltage-dependence of the Mean Open Time.....	50
III-10	: Voltage-dependence of the Frequency of Opening of the Light-activated Channel.....	52



## CHAPTER I

### INTRODUCTION TO THE THESIS

The photoreceptors of the ventral eye of Limulus polyphemus have been one of the most useful preparations for the study of light-transduction. One reason for this is their large size, which make them convenient for electrophysiological studies. Another reason is the arrangement of these photoreceptors in the ventral "eye"; unlike most other photoreceptors, which are organized into networks and are electrically coupled, the ventral photoreceptors have an apparently much simpler organization and many individual photoreceptors are not electrically coupled. This characteristic is important for the study of the electrophysiological properties of individual photoreceptors.

The absorption of light by rhodopsin leads to a change in membrane conductance in the photoreceptor. This transduction process is apparently mediated by a complex series of steps (Fuortes and Hodgkin, 1964; Dodge et al, 1968). Some of the later steps of this process involve amplification (Goldring et al, 1983). Wong estimated that the isomerization of a single rhodopsin molecule activates  $10^3$  light-activated 'channels' in the membrane of a dark adapted Limulus ventral photoreceptor. To explain this gain it has been proposed that this sequence of events controls the concentration of an internal transmitter molecule in the cytoplasm of the photoreceptor (Cone, 1973). The internal transmitter, which has not yet been identified, is thought to interact with the membrane 'channels' underlying the light-activated conductance.

The electrophysiological properties of ventral photoreceptors are relatively well understood at the macroscopic level. By means of the conventional 2-microelectrode voltage-clamp technique (Millecchia and

Mauro, 1969c, Lisman and Brown, 1971a; Fain and Lisman, 1981) various ionic conductances have been characterized. The membrane of this photoreceptor has a conductance that is activated by light as well as various voltage-activated conductances.  $\text{Na}^+$  influx through the light-activated conductance causes the membrane to depolarize, activating the voltage-dependent conductances. The light-induced depolarization is composed of a fast spike followed by a transient depolarizing phase, after which the potential decays to a lower, maintained depolarizing level (Millecchia and Mauro, 1969b). An early inward voltage-activated current carried by  $\text{Na}^+$  and  $\text{Ca}^{2+}$  is responsible for the spike (Lisman et al, 1982). The transient phase is generated by the light-activated inward current (Millecchia and Mauro, 1969c). Repolarization from the transient is due to a combination of factors (Fain and Lisman, 1981): a decrease in the light-activated current due to a  $\text{Ca}^{2+}$ -mediated reduction in the light-activated conductance (light-adaptation); the development of a fast, transient voltage-dependent  $\text{K}^+$  outward current; and a contribution from a slower  $\text{K}^+$ -current associated with separate voltage-dependent  $\text{K}^+$ -channels. This latter  $\text{K}^+$ -current is maintained and, in combination with a maintained component of the light-activated current is responsible for the plateau phase of the receptor potential.

From the macroscopic studies, much information has been obtained about the properties of the conductances underlying the different currents (Fain and Lisman, 1981). The selectivity of them has been studied. Furthermore, study of the kinetics of the currents under various conditions has provided information about the gating properties of these conductances (Fain and and Lisman, 1981). The regulation of

the conductances by different factors has also been studied to some extent (Lisman and Brown, 1972; Leonard and Lisman, 1981; Chinn and Lisman, 1984). However, a question of fundamental importance that has not been answered by macroscopic techniques concerns to the nature of the unitary membrane constituent underlying the light-activated conductance. The currents could be carried either by ionic channels or carriers (Fain and Lisman, 1981). Noise analysis studies in the ventral photoreceptor (Wong, 1978) suggest that ionic channels underlie the light-activated conductance; however, no direct evidence for channels is provided by such studies.

To address this question, a different approach is necessary. Recently, the patch clamp technique for single-channel recording was developed (Neher and Sackmann, 1976; Hamill et al, 1981). This technique makes it possible to measure directly the current passing through individual ionic channels. The method has been used to study the membrane conductances at the molecular level in a number of preparations and has revealed that ionic channels underlie most, if not all conductances. However, in sensory neurons no direct evidence for channels activated by the sensory stimulus has been previously obtained. The major aim of this Thesis was to study this problem in the ventral photoreceptor. By using the patch clamp technique, we sought to study the light-activated conductance at the single-channel level. We found that light activates ionic channels and we give evidence indicating that these channels underlie the macroscopic light-activated conductance (Chapter III).

In order to study the light-activated channel at the 'single-channel' level it was important to have a detailed understanding of the structure of this cell. It is known that many photoreceptor cells have a clear compartmentalization of their cell bodies into a transducing and non-transducing part and both are morphologically and physiologically distinct (Fein and Szuts, 1982). Vertebrate photoreceptors are subdivided into an inner and outer segment. The outer segment is specialized in transduction; it contains the disks, where most of the rhodopsin is located; also the light-sensitive  $\text{Na}^+$  current flows across the membrane of this region of the cell (Hagins et al, 1962; Baylor et al, 1979b), suggesting that the light-sensitive conductance is localized to the outer segment. The inner segment contains the nucleus and all other organelles and apparently does not directly participate in transduction. Similarly, in many invertebrate photoreceptors a clear subdivision has been found in their cell bodies (Fein and Szuts, 1982). They characteristically have micrivilli on part of the plasma membrane, which is called the rhabdome. Rhodopsin is localized to the rhabdome (Langer and Thorell, 1966; Goldsmith et al, 1968), and there is evidence suggesting that the transduction process occurs in this region of the cell (Fein and Szuts, 1982). The cell body of the ventral photoreceptor was also found to have a rhabdome (Clark et al, 1969a), but no obvious compartmentalization of the rhabdome was found in the membrane of this photoreceptor. However, after removing the glial cells surrounding the photoreceptor, we found that the cell body of the ventral photoreceptor is subdivided into lobes. A second major goal of this Thesis was to examine whether these lobes were structurally and functionally different. This study is described in Chapter II.

We found that the rhabdome is compartmentalized to one of the lobes and that this lobe is the light sensitive part of the cell. The light-activated channels were found in the light-sensitive lobe of the photoreceptor.

The identification of many of the various steps of the transduction process is still a distant goal. The work done in this Thesis is a contribution to the understanding of the last of them: the properties of the light-activated conductance.

## CHAPTER II

### Distinct Lobes of Limulus

#### Ventral Photoreceptors.

#### Functional and Anatomical Properties of Lobes Revealed by Removal of Glial Cells

## SUMMARY

1) After mild pronase treatment, the glial cells surrounding the photoreceptor were removed by means of a suction pipette.

2) Observation of such "denuded" cells under the light microscope reveals two kinds of lobes. The "R-lobe" appears translucent whereas the "A-lobe" is more opaque.

3) Scanning electron microscopy of denuded photoreceptors reveals that microvilli (rhabdome) are only present on the R-lobe.

4) Experiments in which the photoreceptor was illuminated with a small spot of light indicate that the light sensitivity of the photoreceptor is localized to the R-lobe.

5) The same kind of experiments shows that light-adaptation is also initiated in the R-lobe of the photoreceptor.

6) It is concluded that the R-lobe is the light-sensitive part of the photoreceptor.



## METHODS

Male Limulus (carapace 15-25 cm) were obtained from Marine Biological Laboratory, Woods Hole, MA. Ventral nerves were removed from the animal under bright white light. Photoreceptors on the ventral nerve were individually denuded of their surrounding glia and connective tissue by the procedure described in Results. The suction pipette used to denude photoreceptors was fabricated as follows. Boralex micropipettes (100  $\mu$ L) were heated and pulled in a 2-stage microelectrode puller in order to produce pipettes with a taper 3-6 mm in length. The tip was cut off by scoring the glass with sandpaper and then breaking off the end. Alternatively, the tips could be melted slightly by contact with a heated platinum filament. Upon cooling, the filament withdrew, producing a clean break in the glass. The tip (at this point 60 to 80  $\mu$ m in diameter) was then brought close to a heated filament until it attained an inner tip diameter of approximately 20  $\mu$ m. The pipette was filled with artificial seawater (ASW) and placed in a micromanipulator joystick or a with a sliding plate. Surface material was removed from the cell, by applying suction to the back of the pipette. During denuding cells were observed through a compound microscope (150X magnification).

In preparation for scanning electron microscopy, denuded photoreceptors were fixed for 1 hour in 2.5% glutaraldehyde. This solution was made by diluting 25% biological grade glutaraldehyde (Electron Microscopy Science, Fort Washington, PA) with concentrated ASW such that the final osmolarity of the solution after dilution was approximately 930 mosm. The preparation was then washed in distilled

water for several hours. In order to dehydrate the preparation it was bathed for 5 minutes in each of the following alcohol solutions: 25%, 50%, 75%, 90%, 95%, and 3 changes in 100% ethyl alcohol. The preparation was then critical point dried from liquid CO<sub>2</sub> in a Bomar SPC-900/EX dryer following standard procedures. For viewing in the scanning electron microscope, specimens were attached to specimen mounts using double-stick-Scotch tape. The specimens were sputter coated (Technics, Hummer II) with gold-palladium to give a coating thickness of about 200A, and they were viewed with an AMR 1000A scanning electron microscope at 20KV.

To measure the responses of denuded cells to small spots of light, cells were held by a suction pipette and impaled with a conventional microelectrode. A spot was made by interposing a pinhole in a light beam. The pinhole was mounted on an X-Y micropositioner so that the spot could be moved. To position the spot without light-adapting the cell, we illuminated the preparation with infrared light and viewed the cell with an infrared image-converter attached to the microscope.

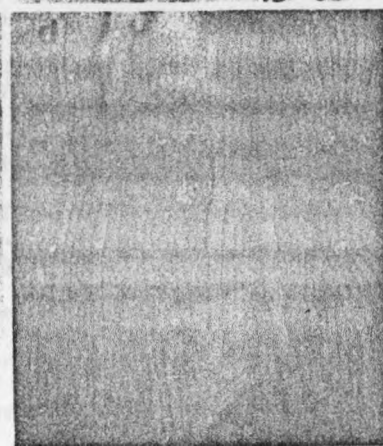
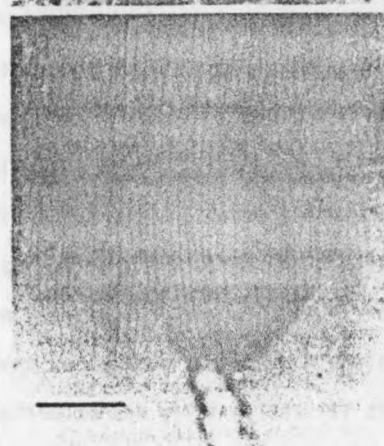
## RESULTS

### A. Denuding the Ventral Photoreceptor

The appearance of two ventral photoreceptors before and after the removal of glial cells and connective tissue is illustrated in Fig. 1. Before denuding, the cells bodies have no obvious substructure (Fig. 1a). After denuding, a subdivision of the cell into lobes is clearly apparent (Fig. 1c).

The method used for denuding cells is as follows: A ventral nerve is desheathed and pinned to a Sylgard substrate. Pronase (Calbiochem, La Jolla, CA; 20mg/ml) is applied at room temperature until the tissue begins to show signs of loosening (approximately 1 minute). The pronase is removed and the tissue is then left undisturbed for an hour in ASW. During this time some of the glial cells that surround the photoreceptor become round. A suction electrode is then used to pull on the connective tissue and glial cells in order to further loosen their connection with the photoreceptor. Then, starting at the axon hillock region, the glial cells and associated connective tissue are progressively peeled away. For this procedure to be successful the photoreceptor must remain anchored to the ventral nerve by its axon. If the pronase treatment is too severe, the axon will easily detach from the ventral nerve and then there is nothing to hold the photoreceptor in place when suction is applied to the glial cells. If the denuding process has gone well, the cells will be firm and resistant to deformation. If the photoreceptors are soft and the cytoplasm appears to have liquified, gentler denuding is required. There is significant variability between animals in the ease of the denuding process.

**FIGURE 1.** Appearance of ventral photoreceptors in the light-microscope before and after removal of glia and connective tissue. a. Two photoreceptors during a very early stage of denuding process. The cell bodies have been pulled away from the ventral nerve (bottom) but are still connected to it by their axons. The suction pipette used for removal of glial and connective tissue is seen at the top of the photograph. b. A cell after denuding. Note that there are two distinct lobes. c. The cell in the right half of Fig. 1a after being denuded. d. A denuded cell with the R-lobe lying to the side of the A-lobe of the cell. The cell's axon, which is out of focus, is attached to the upper left corner of the A-lobe. Calibration bar is in c is  $50\mu$  and applies to the whole figure.

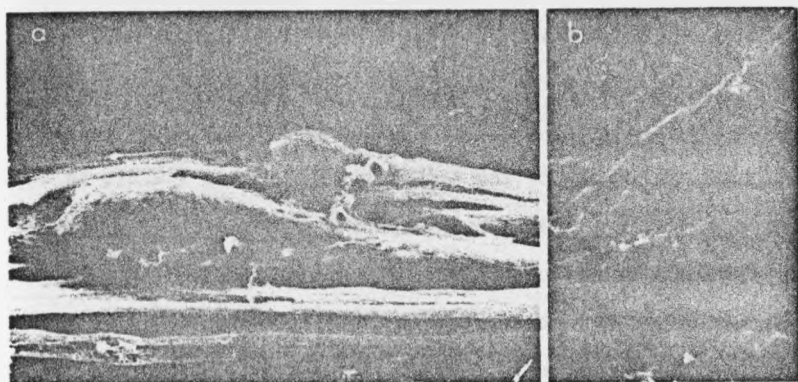


The denuded ventral photoreceptors shown in Fig 1b,c,d have two clearly distinguishable lobes. The lobe most distant from the axon appears somewhat translucent and clear; such lobes are termed R-lobes. The lobes connected to the axon have more texture, and are termed A-lobes. This difference between R and A lobes is usually discernable though it is sometimes less obvious than in Fig. 1b,c,d. The basis for the choice of terminology R (rhabdomeric) and A (arhabdomeric) is given in the companion paper (Calman and Chamberlain, 1982).

The number, shape and position of R-lobes varies considerably from cell to cell, even within the same ventral nerve. Cells with one R-lobe are more common along the ventral nerve than in the cluster of cells at the distal end of the nerve (the end organ). Some cells have two well defined R-lobes (see Fig. 4) and in the end organ, even more complex cells are occasionally seen. In cells with one R-lobe, the R-lobe is usually positioned opposite the axon (as in Fig. 1b,c,), but sometimes the R-lobe lies to the side of the A-lobe (Fig. 1d). Cells with two R-lobes are rarely found as isolated cells but usually as the distal member of a pair of closely opposed photoreceptors. The proximal photoreceptor typically has a single R-lobe at its distal end which is juxtaposed to one of the R-lobes of the distal cell. In pairs or clusters of photoreceptors adjoining R-lobes are strongly attached to each other. To isolate a single cell from a cluster of cells, the neighboring cells must be killed by breaking their membranes. Quite often what initially appears to be a single cell is revealed to be a pair of cells after denuding.

In addition to the variability in the number and position of R-lobes there is considerable variation in their shape. Some R-lobes

**FIGURE 2.** Appearance of cells in scanning electron microscope before denuding. a. Photoreceptor embedded in the ventral nerve. Calibration bar 100  $\mu$ . b. Closeup of fibers that cover glial cells. Calibration bar 1  $\mu$ .





are nearly spherical, as in Fig. 1c, some are conical, and still others form long finger-like projections. There is also variation in cell size. The teasing apart of end-organs during the denuding process reveals a population of small cells, 15 to 25 $\mu$ m in diameter. As judged by extracellular recordings using a suction electrode, at least some of the small cells generate receptor potentials (Stern, unpublished).

#### B. Scanning Electron Microscopy of Ventral Photoreceptors


Cells were examined in the scanning electron microscope (SEM) using the procedure described in Methods. Fig. 2 shows a cell which has not been denuded. The cell is surrounded by a fibrous material; lobes are not apparent. Fig. 3 shows a light micrograph of a denuded cell and a scanning electron micrograph of the same cell. The lobes visible in the light microscope (Fig. 3a) are readily apparent in the scanning electron microscope (Fig 3b) and the surface of the A and R-lobes have a very different appearance. At higher magnification (Fig. 3c) it can be seen that the surface of the R-lobe is covered with microvilli but none are seen on the A-lobe surface.

We have examined 12 denuded cells in the scanning electron microscope. In 6 cells, microvilli were clearly visible. In one such cell there were two R-lobes, both covered with microvilli (Fig. 4). In 6 cells, lobes were clearly distinguishable but microvilli were not observed. It is possible that the lack of microvilli was caused by the denuding process or by the preparation for microscopy. There is often a well defined cleft between R and A-lobes (Fig. 4d) that forms the boundary between the microvillar R-lobe and the smooth surface of the

**FIGURE 3.** Appearance of denuded cell in the scanning electron microscope. a. Light micrograph of a denuded cell having one R-lobe and one A-lobe Calibration bar 25  $\mu$ . b. The same cell seen in the scanning electron microscope. Note that after being denuded the isolated cell (seen in a) was placed on the surface of the ventral nerve. c. Closeup of the R-lobe showing microvilli. Calibration bar 1  $\mu$ .

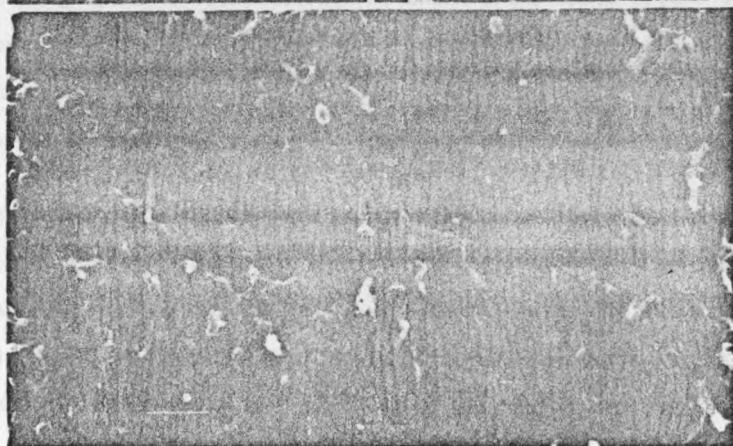
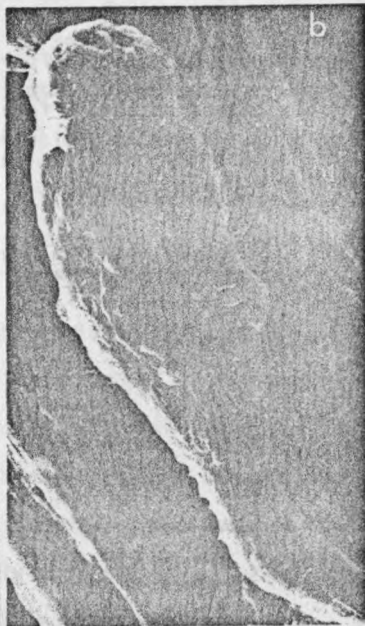
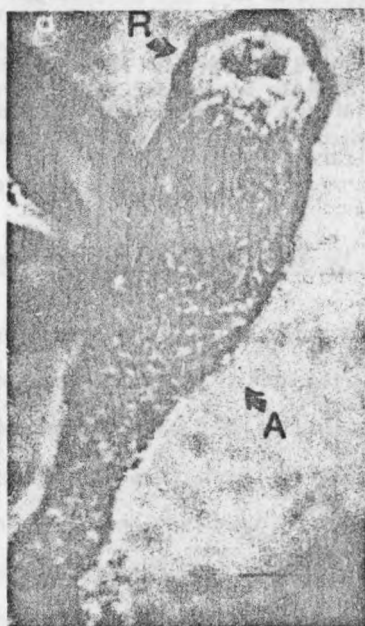
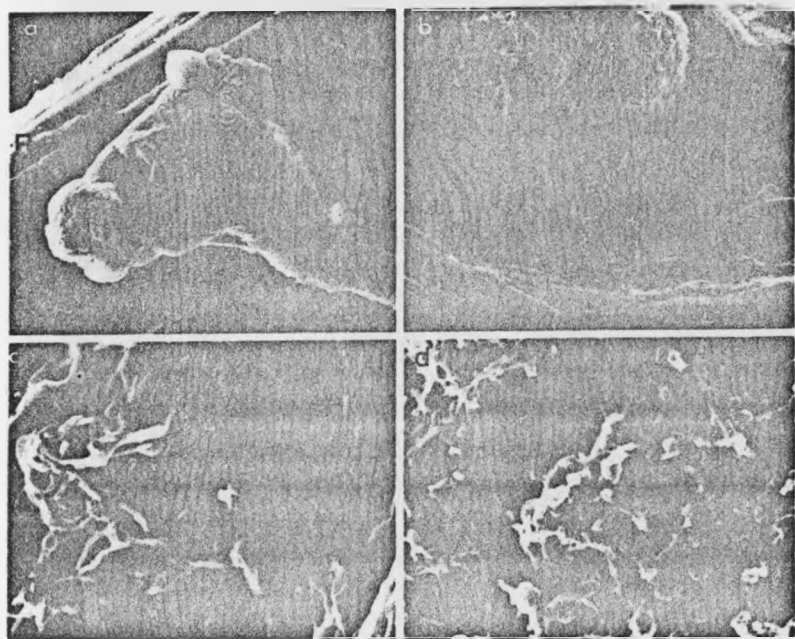


**FIGURE 4.** Scanning electron micrograph of a ventral photoreceptor having two R-lobes and one A-lobe. The two R-lobes are located at the sides of the A-lobe. The smooth bleb seen on the right R-lobe was observed in the light microscope prior to fixation and probably results from local damage. b. Close-up of the junction between the left R-lobe and the A-lobe, showing the invaginations of the membrane in this region. c. Close-up of the left R-lobe showing the microvilli. d. Close-up of the left R-lobe. A calibration bar is shown in b and represents  $48\mu\text{m}$  in a,  $5\mu$  in b,  $2.2\mu$  in c and d.





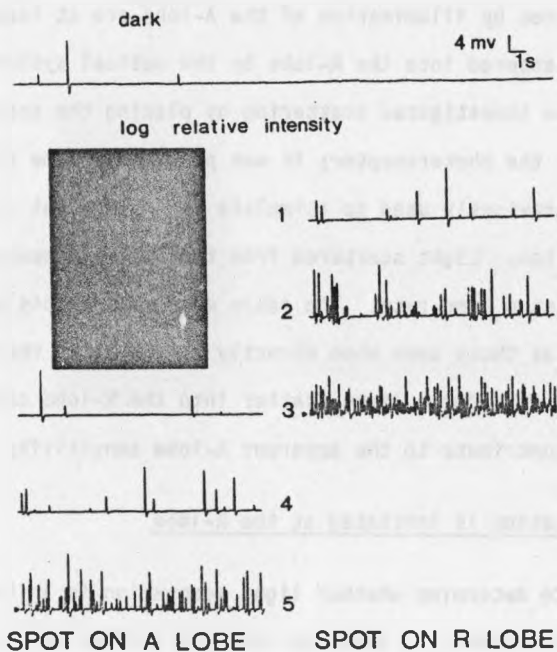
A-lobe. Another interesting feature is the dimpling of the R-lobe surface (Fig. 3b) which may be sites of membrane infoldings.

### C. Sensitivity of the R-lobe and the A-lobe to light

Fig. 5 illustrates an experiment in which we investigated the light sensitivity of the A and R-lobes using a small spot of light (nominal diameter, 10  $\mu$ m). The photograph shows a denuded photoreceptor held by a suction pipette and impaled by a microelectrode to record membrane potential. In all such experiments the A-lobe was impaled. Since the inside of ventral photoreceptors is isopotential (Brown, Harary, and Waggoner, 1979), the potential recorded by the microelectrode is the same regardless of its location. The records show quantum bumps obtained under conditions of illumination which are indicated at the side of each trace. The dark rate is shown in the uppermost trace. When the A-lobe was illuminated by a dim spot (designated "log intensity 3" in Fig. 5), the quantum bump rate was comparable to the dark rate: when the same spot was placed on the R-lobe it caused a dramatic increase in the quantum bump rate. Similarly, over a wide range of intensities, the response was greater when the spot was placed on the R-lobe than when it was placed on the A-lobe.

In order to quantify the difference in sensitivity between the two lobes, the rate of light-evoked quantum bumps was determined by subtracting the spontaneous rate from the total bump rate during illumination. Conditions were selected so that the bump rate was low enough to allow accurate identification of individual bumps. Since the light-evoked quantum bump rate is linearly related to light intensity (Fuortes and Yeandle, 1964), the relative sensitivity (the relative

**FIGURE 5.** Differential sensitivity to light of the A-lobe and R-lobe, inset shows denuded cell held by suction pipette and impaled by a microelectrode. The upper star marks position of the small spot of light used to stimulate the R-lobe. Similarly, a spot at the lower star was used to stimulate the A-lobe. The calibration bar is 25 $\mu$ m. The traces show the changes of membrane voltage recorded by the microelectrode. The uppermost trace has three upward deflections, each of which is a quantum bump. The record indicates that this cell had a low rate of quantum bumps in the dark. The remainder of the traces show the response to light for steady spots placed on the A-lobe (left) or R-lobe (right). The intensity of the spot was increased in 10-fold steps from top to bottom (log relative intensity is given by each trace; absolute intensity was not measure).



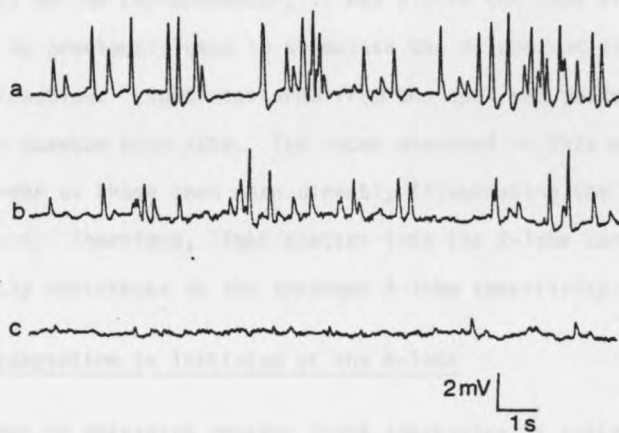


probability of an incident photon evoking a quantum bump) could be directly computed from such measurements. For the cell in Fig. 5 the light sensitivity of the R-lobe was 940 times higher than the A-lobe. In 3 other cells the ratios in light sensitivity between the R and A-lobe were 510, 200, and 87. The true difference in sensitivity between lobes should be higher than what we have measured since responses produced by illumination of the A-lobe are at least in part due to light scattered into the R-lobe by the optical system and by the cell itself. We investigated scattering by placing the spot so that it did not fall on the photoreceptor; it was placed the same distance from the R-lobe as previously used to stimulate the A-lobe but in the opposite direction. Light scattered from the spot was measured as an increase in quantum bump rate. The rates measured in this way were of the same order as those seen when directly illuminating the A-lobe with the same spot. Therefore, light scatter into the R-lobe can significantly contribute to the apparent A-lobe sensitivity.

#### D. Light adaptation is initiated at the R-lobe

In order to determine whether light adaptation is initiated primarily in the R-lobe, an adapting spot was used to stimulate either the A-lobe or the R-lobe selectively (see Fig. 6). Subsequent changes in sensitivity were measured using a dim test spot incident on the A-lobe. Reduction in quantum bump amplitude serves as a measure of the extent of light adaptation (Dodge, Knight, and Toyoda, 1968). After an adapting spot was focused onto the R-lobe there was a much larger reduction of quantum bump amplitude (Fig. 6c) than after placing it on the A-lobe (Fig. 6b). Thus, like excitation, light adaptation is initiated primarily in the R-lobe.

**FIGURE 6.** Effect of position of adapting spot on subsequent sensitivity to light. a. Dark-adapted response to test stimulus spot on A-lobe. b. Response to same test stimulus after adapting light was placed on A-lobe. There was little adaptation. c. Response to same test stimulus after adapting spot was placed on R-lobe. The greatly reduced quantum bump amplitude indicates that substantial light-adaptation occurred.



## DISCUSSION

As illustrated in Figs. 1, 3 and 4, Limulus ventral photoreceptors are subdivided into anatomically distinct lobes. In living preparations these lobes are obvious only after removing the glia that surround the photoreceptors and this helps to explain why the lobes were not previously recognized. The lobes seen in denuded cells are not an artifact created by the denuding procedure since they can be readily identified in sections of intact ventral photoreceptors (Calman and Chamberlain, 1982).

We have shown by scanning electron microscopy that only R-lobes have microvilli on their outer surface. This has been confirmed by Calman and Chamberlain (1982) who have identified microvilli on the outer surface of R-lobes of ventral photoreceptors fixed in vivo for transmission electron microscopy. They further showed that all microvilli are restricted to the R-lobe surface and to deep invaginations of the R-lobe. These invaginations may begin as the dimples seen on the R-lobes (Fig. 3b).

Two features of the microvilli as seen in the scanning electron microscope are unexpected: first, the microvilli appear to be loosely packed, as opposed to the tight packing typical of invertebrate rhabdom and of ventral photoreceptors before denuding (Calman and Chamberlain, 1982); second, the microvilli are sometimes gnarled and fused. Structures of this kind have not been seen in the transmission electron microscope and may be artifacts due to the denuding or fixation processes.

The R and A-lobes are physiologically different. The R-lobe is at least two to three orders of magnitude more sensitive to light than the A-lobe. Microvilli are restricted to the surface of the R-lobe and its infoldings (Calman and Chamberlain, 1982). Since the presence of microvilli greatly increases the membrane area, the high relative sensitivity of the R-lobe to light is expected, even if rhodopsin is uniformly distributed within the membrane. Recent immunological evidence suggests that rhodopsin is present through both the rhabdomeric and non-rhabdomeric membrane of squid photoreceptors (Wong, et al, 1982). Assuming that the A-lobe in Limulus does contain a small amount of rhodopsin, it would be interesting to know whether such rhodopsin can initiate excitation or whether it is silent because it lacks some component associated with the microvillar structure that is necessary for transduction. Unfortunately, technical problems in our experiments make it unclear whether the low but finite sensitivity of the A-lobe is real or whether its apparent sensitivity is an artifact due to light scattered into the R-lobe.

The initiation of light-adaptation also occurs primarily in the R-lobe (Fig. 6). Since light-adaptation in Limulus appears to be mediated by a rise in intracellular free  $\text{Ca}^{2+}$  (Lisman and Brown, 1972; Lisman and Brown 1975) and since  $\text{Ca}^{2+}$  cannot readily diffuse through cytoplasm (Fein and Lisman, 1975), a reasonable expectation would be that the light-induced rise in  $\text{Ca}^{2+}$  would be largest in the R-lobes. Harary and Brown (1981) have shown that the rise in  $\text{Ca}^{2+}$  produced by uniform illumination is spatially nonuniform within ventral photoreceptors, but it is not yet known whether the regions where the increase is large correspond to R-lobes.

Similarly, we do not yet know how excitation processes spread from their site of initiation in the R-lobe. Presumably a diffusable internal transmitter couples the isomerization of rhodopsin to the light-activated channels. From previous work it is clear that the transmitter cannot spread uniformly around the cell: Fein and Charlton (1975) showed that two small spots of light placed at distant regions of a cell produced independent conductance changes that were localized, at least grossly, to the region of illumination. What remains unclear is how far excitation can spread and whether the light-activated channels are in the A-lobe, the R-lobe or both.

### CHAPTER III

#### PROPERTIES OF LIGHT-ACTIVATED CHANNELS

#### IN LIMULUS VENTRAL PHOTORECEPTORS

## SUMMARY

1) The light-activated conductance of Limulus ventral photoreceptors was studied by means of the patch clamp technique for recording single-channel currents.

2) In order to be able to apply the patch clamp technique to this preparation, ventral photoreceptors were denuded from glial cells and mildly sonicated, a procedure that did not alter the physiological properties of the cells.

3) Light activated inward single-channel currents that were absent in the dark.

4) This activity was not induced by depolarization in the dark; therefore, the activation of the channels was not a secondary result of the light-induced depolarization.

5) The single channels activated by light have a conductance of 41pS and a mean open time of 4.1ms.

6) Injection of EGTA into the photoreceptors enhanced the light-induced channel activity. Since EGTA prevents the normal rise in intracellular  $\text{Ca}^{2+}$  normally produced by light, this observation indicates that activation of the channels is not mediated by  $\text{Ca}^{2+}$ .

7) The single-channel conductance is independent of voltage. However, the mean open time and the frequency of opening of the channel depended on voltage, in a manner consistent with the voltage-dependence of the macroscopic light-activated conductance.

8) The reversal potential of the single-channel currents was  $\sim +10\text{mV}$ , in the same range of the reversal potential of the macroscopic light-activated current.

9) Single-channel activity was graded with light intensity, in a way qualitatively similar to the macroscopic light-activated conductance.

10) When a maintained light stimulus was applied, the single-channel activity was initially high and then decayed to a lower and maintained level. This time course qualitatively resembled the waveform of the macroscopic light-activated current.

11) The single-channel activity adapts to light in a qualitatively similar manner as the macroscopic response to light.

12) The evidence indicates that light activates ionic channels in the ventral photoreceptors and that these channels are those which underlie the macroscopic light-activated conductance.



## METHODS

### The Preparation

Horseshoe crabs (Limulus polyphemus) were obtained from the Marine Biological Laboratories, Woods Hole, MA. Ventral nerves were dissected out of the animals, desheathed and pinned down onto the sylgard bottom of the experimental chamber. The nerves were then treated with 2% Pronase (Calbiochem, La Jolla, CA) for approximately 1 min. In order to provide access of the patch clamp pipette to the photoreceptor plasma membrane, the glial cells surrounding the individual photoreceptor were removed by teasing the glia away with a suction pipette of 20  $\mu$ m tip diameter, as described in Stern et al (1982). To be able to orient the cell optimally for recording it was necessary to separate several millimeters of the photoreceptor axon from the ventral nerve.

The cell body of the ventral photoreceptor is subdivided into lobes that are distinct in structure and function (Bacigalupo et al, 1981, Stern et al, 1982). The R-lobe is the light-sensitive part of the cell. It has microvilli on its surface, some of which are on the surface (external microvilli) and others are located in clefts of the plasma membrane (internal microvilli; see Calman and Chamberlain, 1982). The A-lobe has a smooth surface with no microvilli on it and does not appear to be sensitive to light (Stern et al, 1982). We were easily able to obtain patch-clamp current recordings from the A-lobe. However, none of the channels in the A-lobe were directly affected by light. It was therefore desirable to record from the R-lobe of the cell. Using the same approach successfully applied to the A-lobe, we obtained seals on the R-lobe but only after applying considerable suction. The currents

measured from these patches contained a sporadic noise that was independent of light and voltage and was probably due to damage to the patch membrane caused by the high suction. In order to obtain better seals on the R-lobe, further methods of treating the cells were explored. We found that mild sonication of the preparation enabled us to obtain seals on the R-lobe with less suction and to make recordings in which the sporadic noise was usually absent. On the A-lobe, ~80% of the attempts ( $N = 44$ ) to obtain seals were successful (noise level compatible with single-channel current recordings). No successful seals were obtained on the R-lobe of non-sonicated cells ( $N = 28$ ). On the R-lobe of sonicated cells, 43% of the attempts (420) were successful. Of these patches, 16 contained light-activated channels.

To do the sonication, the chamber containing the ventral nerve was covered with a microscope slide and wrapped with parafilm to prevent leakage of water from the sonicator into the chamber. The chamber was then suspended into the sonicator (model G112SP1T, La. Supply Co. Inc., Hicksville, NY), which was set at 80V for 2 min. After sonication photoreceptors were denuded as described above. The function of photoreceptors was not markedly affected by the sonication. Their resting potential was  $48.2 \pm 14.7\text{mV}$  ( $N = 67$ ), near the normal value ( $-40$  to  $-70\text{mV}$ ; Fain and Lisman, 1981), they produced normal light responses (Fig. 2a) and they maintained their ability to respond to single photons (Fig. 4). It is not certain how sonication affected our ability to obtain good seals but it probably altered the R-lobe surface so that areas of it became appropriate for obtaining seals. Preliminary studies of a few sonicated photoreceptors in the scanning electron microscope indicate that the cells did not have external microvilli; however, this

was also sometimes the case for nonsonicated denuded photoreceptors (Stern et al, 1982). Further work will be necessary in order to understand the role of sonication in our experiments. Although the cells, as viewed in the light microscope, were not noticeably affected by sonication, there were some indications that sonication indeed did something to the preparation. First, small vesicles appeared in the bath after sonication, which were never observed in unsonicated preparations. Secondly, photoreceptors of preparations that were exposed to a more prolonged sonication (4 min. or more) occasionally had their axons sectioned into several pieces. Finally, it is our impression that sonicated photoreceptors were easier to denude.

#### The Experimental Apparatus

The denuding procedure and the positioning of the electrodes was done under a compound microscope (MicroZoom, Baush and Lomb, Rochester, NY). This microscope has a long working distance and a zoom feature, which was very convenient because it made it unnecessary to change objectives during the course of an experiment. The denuding of the photoreceptors was done under low magnification (115X) while the positioning of the patch pipette was done under 2-fold higher magnification. The denuding pipette was mounted on a sliding micromanipulator (Stern et al, 1982). This pipette was replaced by a microelectrode after the stripping procedure was completed. The patch pipette was mounted on the second micromanipulator (Line Tool Co., Allentown, PA), which was driven by miniature motors (motor mike, Ardel Kinamatic Corp., College-Point, NY).

The denuding procedure was done under red light. The stimulating light (520nm) had a maximal intensity ( $I_0$ ) of  $\sim 1.4 \times 10^{14}$  photons  $\text{cm}^{-2} \text{s}^{-1}$  at the level of the preparation. The intensity of the light ( $I$ ) was controlled with neutral density filters and is expressed as relative light intensity ( $\log I/I_0$ ).

#### Patch clamp recording

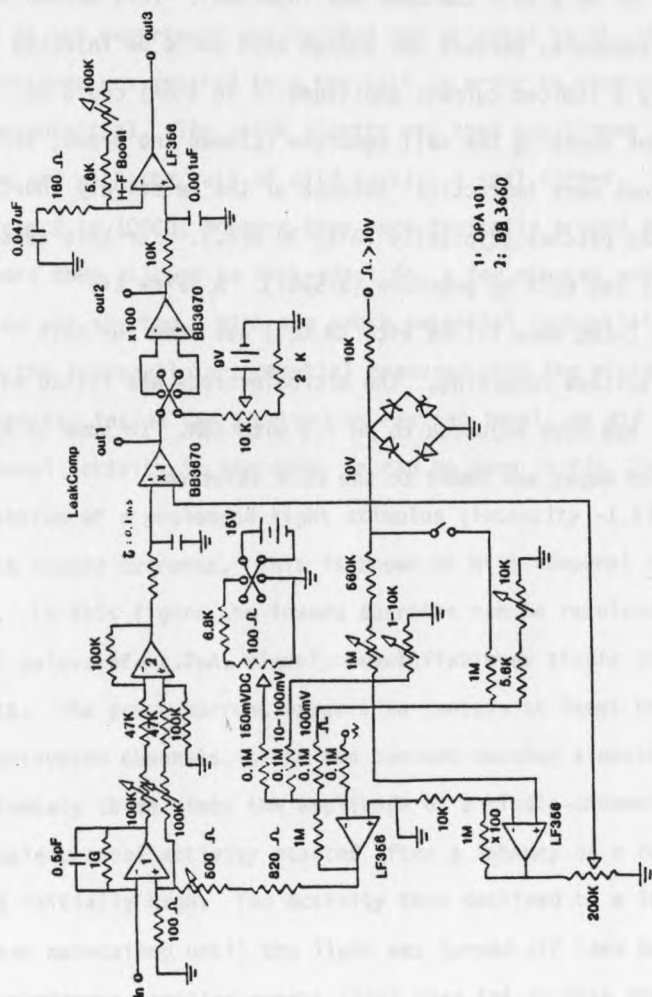
The techniques used for patch clamping were standard (Neher and Sakmann, 1976; Hamill et al, 1981). Pipettes  $\sim 0.5 \mu\text{m}$  were coated with sylgard, firepolished and filled with artificial sea water (ASW). The bath also contained ASW. The composition of the ASW was, in mM: 425 NaCl, 10 KCl, 10  $\text{CaCl}_2$ , 22  $\text{MgCl}_2$ , 26  $\text{MgSO}_4$ , 15 Tris-Cl; pH adjusted to 7.8 with NaOH. A silver/silver chloride electrode was connected to the bath through an ASW-agar bridge. A diagram of the patch-clamp circuit is shown in Fig. 1. Recordings were stored on magnetic tape (model 3964A of Hewlett Packard). Signals were filtered using a 4 pole Bessel filter (model 4302 of Ithaco, Ithaca, NY) set at the bandwidths indicated in the figure legends.

In most of the patch-clamp experiments, an intracellular microelectrode was used to record the membrane potential. The microelectrodes were filled with 3M KCl and had resistances of  $\sim 10 \text{M}\Omega$ , except when otherwise indicated.

#### EGTA injections

In some experiments the intracellular microelectrode was used to inject EGTA [(Ethylenebis(oxyethylene-nitrilo)tetraacetic acid (Eastman, Rochester, NY). Two different injection procedures were tried. In some

**FIGURE 1.** Diagram of the patch-clamp circuit. The operational amplifiers used in the circuit are listed in the bottom right of the figure. The time constant of the circuit was 0.8ms when the input of the amplifier was connected to ground with a dummy made of a  $1G\Omega$  resistor in parallel with a 10pF capacitor (the value of the stray capacitance when the circuit was connected to the whole experimental apparatus). The noise in these conditions was 0.4pA (P-P) when the current was filtered with a Bessel filter (see Methods) set at 1KHz.



experiments we injected the EGTA iontophoretically. In this case, the microelectrode was filled with 300mM EGTA, adjusted to pH 7.0 with KOH. Negative (hyperpolarizing) current was passed through the electrode (until a total of  $\sim 6 \times 10^{-6}$  Coulombs was injected). This method was found to be inadequate, because not enough EGTA could be injected into the cell. Only a limited current amplitude (2 to 3 nA) could be injected without damaging the cell membrane (Lisman and Brown, 1975) and longer injections were impractical because of the relatively short life-time of the patches (typically 20 to 30 min.). For this reason we chose to inject the EGTA by pressure (2-5psi). A large tip microelectrode ( $\sim 1\text{M}\Omega$  when filled with 3M KCl) was used for EGTA injection and voltage recording. The microelectrode was filled with 1.5M EGTA that had been adjusted to pH 7.2 with KOH. In some of the experiments, 7mM Hepes was added to the EGTA solution.

## RESULTS

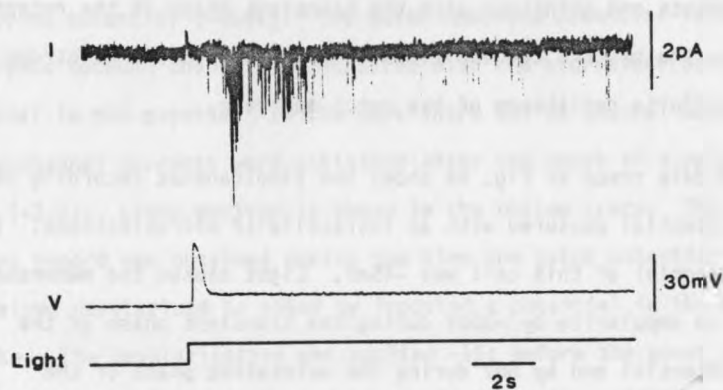
### A. Activation of Single-channel Currents During Illumination.

After sonicating the preparation, the individual photoreceptor to be used in the experiment was denuded and oriented in the chamber. A microelectrode was impaled into the cell in order to measure the membrane potential. The patch pipette was then positioned on the R-lobe membrane and with the help of mild suction a seal formed. We obtained seals from 2 to 100G $\Omega$ ; however they were typically around 20G $\Omega$ . The cells were then allowed to dark-adapt for a few minutes and the recording was started. With the patch potential (potential difference between the intracellular potential measured with the microelectrode and the potential inside the pipette) at resting level, we did not observe any channel activity in the dark, as can be seen in Fig. 2a. Presentation of a prolonged light stimulus (intensity  $-1.6$ ), induced discrete inward currents. This is shown at high temporal resolution in Fig. 2b. In this figure the inward currents can be resolved as discrete current pulses of  $\sim 1.7$ pA, clearly identifiable as single channel currents. The patch current appears to contain at least three light-activated channels, since the current reached a maximum level of approximately three times the amplitude of a single-channel current. The single-channel activity started after a latency of a few hundred ms and was initially high. The activity then declined to a lower level, which was maintained until the light was turned off (see below). In some experiments, smaller events (less than 1pA in this example), occurred infrequently during illumination (see arrows in Fig. 2b). These events appeared to be light-activated, but were so infrequent that we cannot be certain about this.

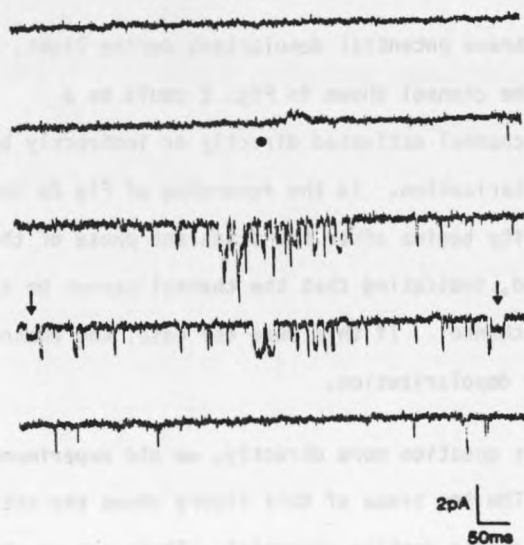


**FIGURE 2.** a. Top trace illustrates a single-channel response to a -1.6 light. The receptor potential of the cell, recorded simultaneously with an intracellular microelectrode, is shown in the bottom trace. The light monitor trace indicates the moment a maintained light was applied to the preparation. The microelectrode ( $10\text{M}\Omega$ , filled with  $3\text{M KCl}$ ) was impaled into the photoreceptor before positioning the patch pipette on the R-lobe membrane, because otherwise the oscillation of the microelectrode used to penetrate the cell would brake the seal. b. High temporal resolution recording of the current trace shown in part a. The traces are a continuous recording initiated in the dark. The dot indicates the moment of the onset of a maintained light (intensity -1.6). The arrows point to two unusually small current channels which appear in our recordings with very low frequency. The recordings were filtered at  $\tau = 0.8\text{ms}$ . Temperature:  $21^{\circ}\text{C}$ .

a



b



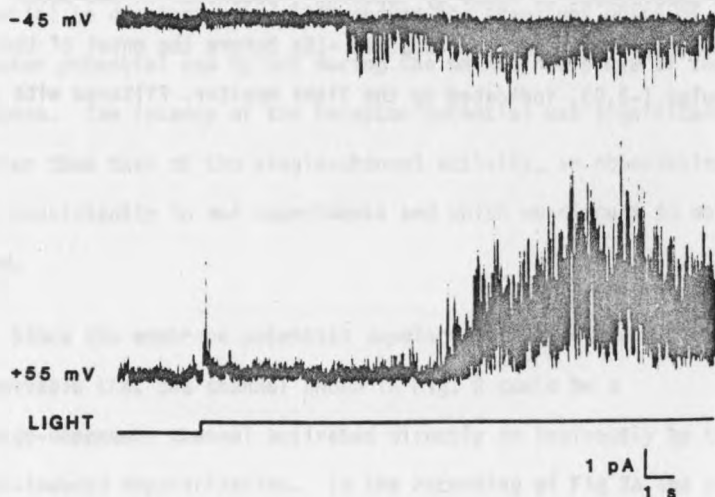
A small outward patch current was observed shortly after the onset of the light stimulus. This early outward current was seen in all of our experiments and coincided with the transient phase of the receptor potential. The outward current flows towards the pipette electrode across the finite resistance of the patch membrane.

The middle trace of Fig. 2a shows the simultaneous recording of the membrane potential measured with an intracellular microelectrode. The resting potential of this cell was  $-45\text{mV}$ . Light caused the membrane potential to depolarize by  $\sim 30\text{mV}$  during the transient phase of the receptor potential and by  $6\text{mV}$  during the maintained phase of the response. The latency of the receptor potential was significantly shorter than that of the single-channel activity, an observation that we made consistently in our experiments and which we discuss in more detail below.

Since the membrane potential depolarizes during light, it is conceivable that the channel shown in Fig. 2 could be a voltage-dependent channel activated directly or indirectly by the light-induced depolarization. In the recording of Fig 2a the period of high channel activity begins after the transient phase of the receptor potential has ended, indicating that the channel cannot be a classic voltage-dependent channel. If this were the case, the channel activity would parallel the depolarization.

To address this question more directly, we did experiments like that shown in Fig. 3. The top trace of this figure shows the activation of channels by light at the resting potential. There was no channel activity before presentation of the light, but single-channel currents

**FIGURE 3.** Light-induced depolarization does not mediate the channel activity. The top trace was obtained while the patch was approximately at resting potential ( $-45\text{mV}$ ). The patch membrane potential is the difference between the voltage measured with the microelectrode and the potential in the pipette. In the dark there was no channel activity. Single-channel currents were activated after the onset of a maintained light ( $-3.0$ ). Light monitor is shown in the bottom trace. The lower current record was obtained during the time the patch potential was maintained depolarized to  $+55\text{mV}$  by imposing a potential in the patch pipette. The depolarization was applied  $\sim 15\text{s}$  before the onset of the light stimulus ( $-3.0$ ), indicated by the light monitor. Filtered with a  $\tau = 0.8\text{ms}$ .



were induced during subsequent illumination (intensity  $-3.0$ ). The voltage in the pipette was zero and therefore the voltage across the patch membrane was resting potential ( $-45\text{mV}$ ) during the dark and slightly depolarized (by  $6\text{mV}$ ) during the maintained phase of the receptor potential. The patch was then depolarized in the dark by changing the potential inside of the pipette. Depolarization of the patch to  $+55\text{mV}$  did not induce channel activity in the dark (bottom trace of Fig. 3), indicating that the activation of the channels was directly light-dependent and was not due to the voltage change. While maintaining the patch depolarized, the cell was stimulated again with the same light. Illumination induced single-channel currents. The single-channel currents were now outward because the patch potential was more positive than the reversal potential for the light-activated current ( $0$  to  $+20\text{mV}$ ; Millecchia and Mauro, 1969; also see below).

The patch of Fig. 3 contained only light-activated channels. However, in some of the patches containing light-activated channels there were also voltage-dependent channels not activated directly by light. The presence of these channels was revealed when the patch potential was varied in the dark. The currents associated with voltage-dependent channels were clearly distinguishable from the light-activated channel currents because they were activated by depolarization and because the direction, magnitude and mean open time were very different from that of the light-activated channel.

#### B. Intensity- and Time-dependence of the Single-channel Activation.

The magnitude of the macroscopic light-dependent current increases when the light intensity is raised (Millecchia and Mauro, 1969b; Lisman

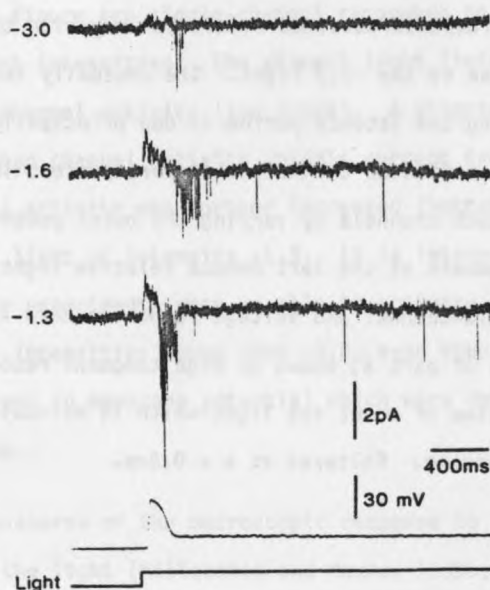
and Brown, 1971a). This was also observed in the activation of the light-activated channels, as illustrated in Fig. 4. The current traces shown in this figure are single-channel responses to light-stimuli of three different intensities. The dimmest light (intensity -3.0) produced low channel activity (top trace). A brighter stimulus (-1.6) induced a higher channel activity (middle current trace). The single-channel activity was further increased (bottom current trace) in response to a light of intensity -1.3. It is interesting to note that in none of our experiments were we able to activate the light-activated channels with intensities lower than -3.0, even though such dim lights produced changes in membrane potential which were detected with a microelectrode.

The time-course of the macroscopic response to light depends on the intensity of the light (Millecchia and Mauro, 1969b; Lisman and Brown, 1971a). Illumination of the photoreceptor with a prolonged dim light stimulus evokes a constant inward current. However, the inward current in response to a bright prolonged stimulus consists of a large initial transient that decays to a lower maintained value. Similarly, the activation of the light-activated channels (Fig. 4a) showed an initial burst of high channel activity which decayed to a lower level that was maintained until the the light was turned off. Results of this kind were obtained in all but one of our experiments. In this one experiment we observed a transient increase in channel activity after termination of the light, which gradually decayed to the dark level (no activity). This post-light activation was not seen in the response to dimmer stimuli. Interestingly, of all the patches that we studied, this patch

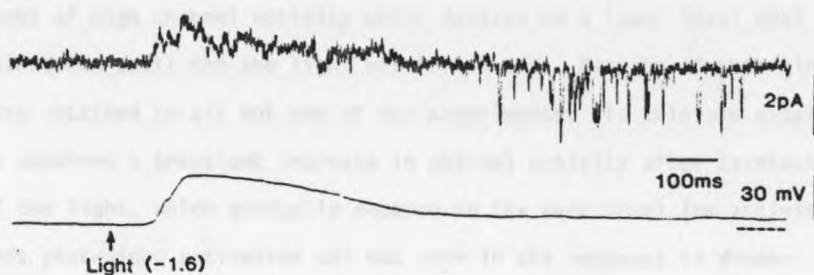
**FIGURE 4.** a. Single channel responses to light-stimuli of increasing intensities. Top trace is the response to dimmest light. At the bottom is shown the voltage response obtained simultaneously with the single-channel response to the -1.3 light. The unusually large outward current observed during the latency period is due principally to the activation of voltage-activated channels that were present in this patch. We resolved such channels by varying the patch potential in the dark (not shown). Numbers at the left denote relative light intensities. b. Single-channel and voltage responses to a -1.6 light (same as middle trace of part a) shown at high temporal resolution. Arrow indicates the time of onset the light which is maintained during the time of this recording. Filtered at  $\tau = 0.8\text{ms}$ .



a



b



presented the highest sensitivity to light (highest channel activity for the given light intensity).

The latency period that preceeds the macroscopic response of the cell is no longer than 150ms and is reduced as light intensity is increased (Millecchia and Mauro, 1969b). A latency also preceeds activation of the light-activated channels. In all our experiments the latency was significantly reduced with bright lights by 5 to 10-fold (see Fig. 4a). However, in our patches we consistently observed latencies that were longer than the macroscopic response typically by a few hundred ms. Fig. 4b shows the top current trace of Fig. 4a expanded in the time scale. In this case the macroscopic response had a latency of ~70ms, whereas the latency of the single-channel response was ~800ms. In all but one experiment the latencies of the single-channel responses were in the range of 60 to 800ms, depending on the patch, the light-intensity and the state of dark-adaptation of the cell. In one patch, the latency of the single-channel response to a dim stimulus was ~4s (top trace of Fig. 3). This was the most extreme case in this regard. At bright light (-1.0) the latency was reduced to 300ms. Interestingly, in order improve the seal on that occasion we needed to apply some extra suction, which might explain this unusually long latency (see Discussion). In conclusion, the activation of the light-activated channels is qualitatively similar to the macroscopic light-activated current in its intensity-dependence and time-course, but has important quantitative differences.

#### C. Effect of Light Adaptation on the Single-channel Response.

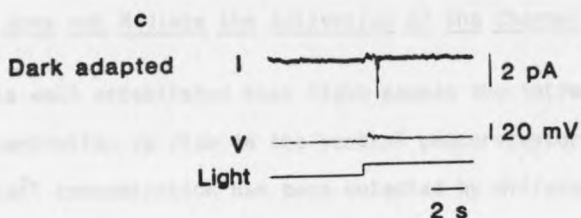
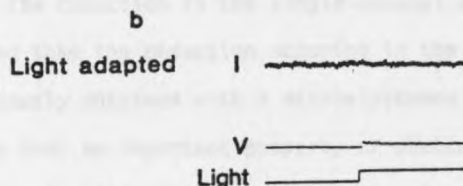
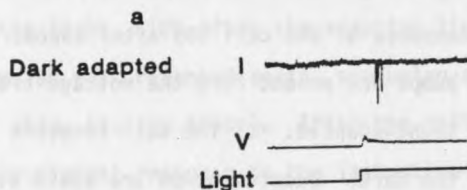
Photoreceptors adapt to light. This means that the response of a

photoreceptor to a light stimulus is reduced in amplitude if the cell has been previously exposed to an adapting light. The experiment in Fig. 5 shows that the same effect of bright light is observed at the single channel level. The single-channel activity evoked by stimulating the dark-adapted photoreceptor with a test light (intensity -3.0) is shown in part a of the figure (top trace). The cell was then exposed to an adapting light. 10s after the adapting light was turned off, the test stimulus was presented again, producing a reduced single-channel activity (Fig. 5b, top trace). After the cell dark adapted for 3 min, the single-channel response to the last stimulus recovered (Fig. 5c, top trace). The reduction in the single-channel activity was more pronounced than the reduction occurring in the voltage response simultaneously obtained with a microelectrode (Fig. 5). This experiment indicates that an important property of photoreceptors, light adaptation, is also evident in the activation of the single-channels.

D. Ca<sup>2+</sup> does not Mediate the Activation of the Channel by Light.

It is well established that light causes the intracellular free Ca<sup>2+</sup> concentration to rise in the ventral photoreceptor. This transient rise in Ca<sup>2+</sup> concentration has been detected by different methods (Brown and Blinks, 1974; Brown et al, 1977; Levy and Fein, 1984). Ca<sup>2+</sup> has been shown to affect the gating of certain ionic channels (Yellen, 1982; Maruyama and Petersen, 1982; Latorre et al, 1984). Although there has been no previous indication of a Ca<sup>2+</sup>-activated macroscopic conductance in Limulus (Fain and Lisman, 1981), we examined the possibility that the light-dependent rise in Ca<sup>2+</sup> could mediate the activation of the channel that we have studied. In these experiments we injected the

**FIGURE 5.** Effect of an adapting light on the single-channel response. The same light (-3.0) is used as a test stimulus in a, b and c. Top traces are patch current recordings. Middle traces are membrane potential recordings obtained simultaneously with the corresponding current traces. a. Response of the dark-adapted cell. State of dark-adaptation is revealed by the quantum bump responses preceeding the onset of the stimulus. b. Response of the cell 10s after exposure to an adapting light. Quantum bumps are absent from the voltage trace, indicating that the cell is light-adapted. c. The cell recovers its response after 3 minutes in the dark. Quantum bumps are again evident in the voltage trace.



$\text{Ca}^{2+}$ -chelator, EGTA, into the photoreceptor and compared the single-channel responses to light before and after the injection. EGTA has been previously shown to abolish the light-induced rise in intracellular  $\text{Ca}^{2+}$  (Brown and Blinks, 1974). Furthermore, the light-adaptation process is  $\text{Ca}^{2+}$ -dependent. For this reason, EGTA drastically increases the amplitude of the steady-state phase of the macroscopic light-activated current. Therefore, a higher steady-state channel activity is expected to occur in the presence of EGTA if the channels we have studied underlie the macroscopic light-activated conductance. On the other hand, if the channel is  $\text{Ca}^{2+}$ -activated, injecting EGTA should depress the activation of the channel by light. The results of EGTA-injections are shown in Fig. 6. EGTA was pressure-injected into the cell with a microelectrode, as explained in Methods. The single-channel recording began a few minutes after the impalement of the cell. In order to compensate for the drop in driving force for the single-channel current that occurs during the large maintained receptor potentials in EGTA-injected cells, a hyperpolarizing potential was applied to the patch a few seconds before the onset of each light stimulus and was maintained during the light. In this particular experiment, a 50mV hyperpolarizing step was applied, which was the amplitude of the receptor potential during the steady-state. Three sequential stimuli were given at intervals of ~1min. Each of the three stimuli evoked similar responses, one of which is shown in the top trace of Fig. 6. During the 1 minute dark period preceeding a fourth light stimulus, EGTA was injected. The response to the following stimulus is shown in the second trace of Fig. 6. The single-channel activation by light was greater than before the EGTA-injection.

**FIGURE 6.** Effect of EGTA on channel activation. Patch current responses obtained before EGTA and after successive EGTA-injections are shown. EGTA was contained into the voltage-measuring microelectrode and pressure-injected into the photoreceptor by applying 3 to 5psi for ~5s to the back of the microelectrode. The patch recording started a few minutes after the impalement of the microelectrode. The light stimuli of intensity -1.0 were applied at intervals of 1 min. However, some leak of EGTA into the cell during that time was evident from the shape of the voltage response to light (not shown), which had large steady-state level characteristically produced by EGTA. Each stimulus was repeated three times between each injection. ~5s before each stimulus, the patch was hyperpolarized by 60mV and the hyperpolarization was maintained until after the offset of the light. The purpose of this imposed potential was to compensate for the drop in the driving force for the light-activated current during the light-induced depolarization, which was of approximately 40mV. The channel activity was reduced by the subsequent repetitive stimuli after each injection, although only one example of this is shown here (after the second injection, bottom current trace). This patch contained voltage dependent channels, in addition to the light-activated channels. Current filtered at  $\tau = 0.8\text{ms}$ .

**Before  
Injection**



**1st  
Injection**



**2nd  
Injection**

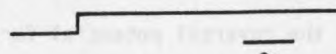


**2pA**

**After  
Several  
Stimuli**



**Light**



**2s**



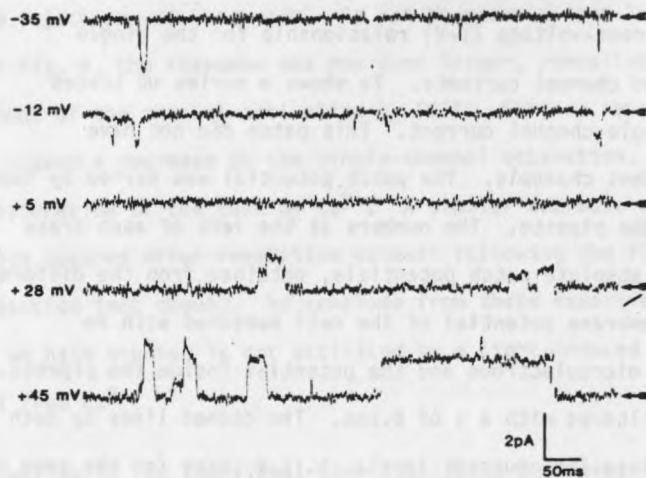
A second injection was then made. As can be clearly seen in the third trace of Fig. 6, the response was now even larger, revealing further enhancement of the channel activation by EGTA. Further repetitive light stimuli caused a decrease on the single-channel activation, presumably due to saturation of the EGTA by  $\text{Ca}^{2+}$ . A similar decrease of channel activation occurred after repetitive stimuli following the first EGTA-injection (not shown). We conclude from these experiments that the channel we have studied is not activated by a light-induced rise in internal free  $\text{Ca}^{2+}$ .

#### E. Properties of the Individual Light-activated Channels.

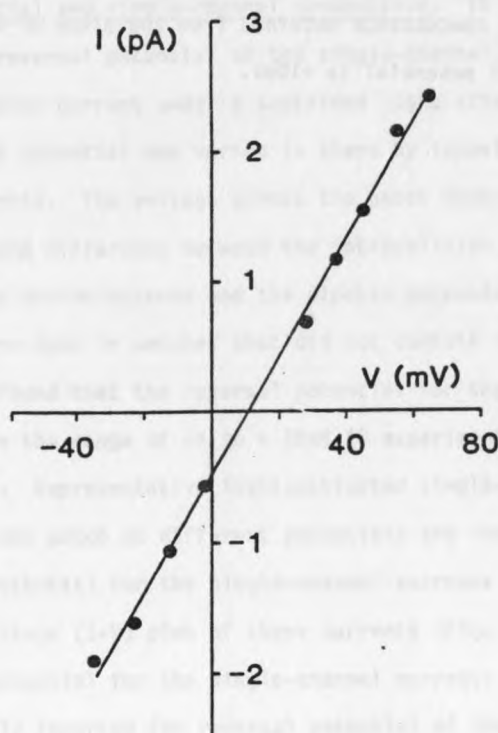
Reversal potential and single-channel conductance. In order to determine the reversal potential of the single-channel currents, we recorded the patch current under a sustained light stimulus, during which the patch potential was varied in steps by imposing potential inside the pipette. The voltage across the patch membrane was calculated as the difference between the intracellular potential measured with a microelectrode and the pipette potential. These experiments were done in patches that did not contain voltage-dependent channels. We found that the reversal potential for the light-activated currents was in the range of +5 to +19mV (5 experiments; average:  $9 \pm 3$  (s.e.m.) mV). Representative light-activated single-channel currents obtained from one patch at different potentials are shown in Fig. 7a. The reversal potential for the single-channel currents was obtained from the current-voltage (I-V) plot of these currents (Fig. 7b) and is +10mV. The reversal potential for the single-channel currents is within the range previously reported for reversal potential of the macroscopic

**FIGURE 7.** Current-voltage (I-V) relationship for the single light-activated channel currents. 7a shows a series of traces containing single-channel current. This patch did not have voltage-dependent channels. The patch potential was varied by imposing a voltage in the pipette. The numbers at the left of each trace correspond to absolute patch potentials, obtained from the difference between the membrane potential of the cell measured with an intracellular microelectrode and the potential inside the pipette. The traces were filtered with a  $\tau$  of 0.8ms. The dashed lines by each trace indicate the base-line current level. b. I-V curve for the same data as in part a. The straight line was fitted by the least squares method. The single channel conductance obtained from the slope of the curve is 45pS. The reversal potential is +10mV.

a



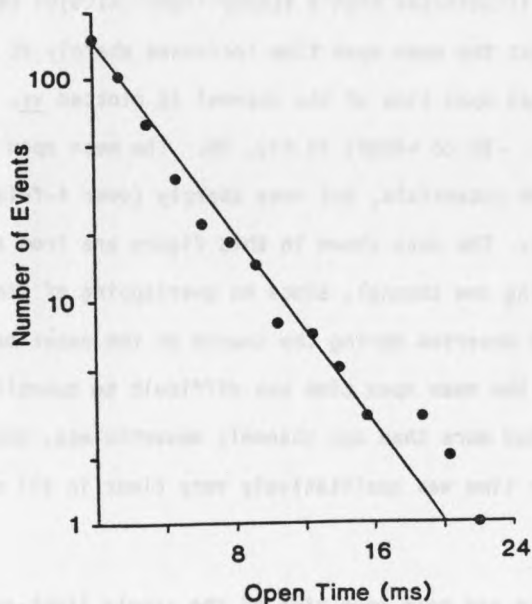
b



light-activated current: 0 to +20mV (Millechia and Mauro, 1969c; Brown and Mote, 1974). The conductance of the individual channel, calculated from the slope of the I-V curve, is 45pS. The average value for the single-channel conductance (5 experiments) is  $41.2 \pm 5.2$  (s.e.m.) pS. The I-V relationship of the light-activated channel is linear within the voltage range we used, indicating that the conductance of the single channel does not depend on the membrane potential. Although a systematic study in a single patch was not done, measurements of conductance in 5 separate patches at various light intensities suggest that the single-channel conductance does not have an obvious dependence on light intensity.

Single-channel mean open time. The mean open time of the light-activated channel was obtained from the distribution of open times (Fig. 8). The photoreceptor was illuminated with a steady light (-1.0), while the patch potential was -35mV. The experiment was performed at room temperature (21°C). The measurements of the open times were done during the steady-state phase of the response. Some of the events were too fast to be well resolved by our system, which had a  $\tau = 0.8$ ms. The longer individual events reached an amplitude of 1.8pA (not shown). We chose to measure the 'width' of the events (i.e. the open time) at 1/2 this value (0.9pA) from the baseline. Events with an open time  $< 0.55$ ms were then below the limit of resolution that we established and, therefore, were ignored. Each experimental point in the plot represents the sum of the events with a duration  $> t$ , (total number of events = 145). The points were best fitted with a single exponential of time constant,  $\tau$ , of 4.7ms, which corresponds to the mean open time of the channel. The value of the mean open time calculated as the average of

**FIGURE 8.** Semilog plot of the distribution of open times of single light-activated channels. The experimental points (total of 145 events) were best fitted by a single exponential of  $\tau = 4.7\text{ms}$  and represent the number of single-channel events with a duration  $>t$ . The open times were measured during a light of intensity  $-1.0$  and a steady absolute patch potential of  $-35\text{mV}$  (difference between the potential inside the cell, measured with an intracellular microelectrode, and the potential inside the pipette). The open time for this channel calculated as the average of the 145 events was  $4.1 \pm 0.5\text{ms}$ . The current was filtered with a  $\tau = 0.8\text{ms}$ . Temperature:  $21^{\circ}\text{C}$ .



the 145 events was  $4.1 \pm 0.5$  (s.e.m.) ms for the channel in this patch. The average value for the mean open time measured in 11 experiments is  $3.0 \pm 0.4$  (s.e.m.) ms. These measurements were obtained at different light intensities (-3.0 to 0) and the mean open time did not have any obvious dependence on the intensity.

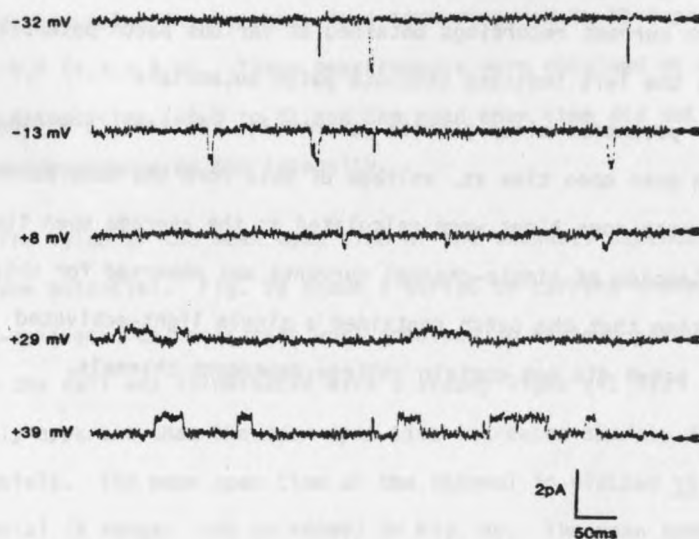
The value of the mean open time of the channels depended on membrane potential. Fig. 9a shows a series of current traces containing light-activated channels that were obtained at various patch potentials while the cell was illuminated with a steady light (-1.3). It is readily apparent that the mean open time increases sharply at positive potentials. The mean open time of the channel is plotted vs. the patch potential (V range: -35 to +40mV) in Fig. 9B. The mean open time was near 4ms at negative potentials, but rose sharply (over 4-fold) at positive potentials. The data shown in this figure are from a patch apparently containing one channel, since no overlapping of single channel events were observed during the course of the experiment. In all other patches, the mean open time was difficult to quantify because the patches contained more than one channel; nevertheless, the effect of voltage on the open time was qualitatively very clear in all such cases.

The conductance and mean open time of the single light-activated channel were apparently not altered after injection of EGTA into a cell. We were able to measure these values in one patch from an EGTA-injected cell and obtained a single-channel conductance of 37pS and a mean open time of 3.1ms, both within the same ranges measured in uninjected photoreceptors.

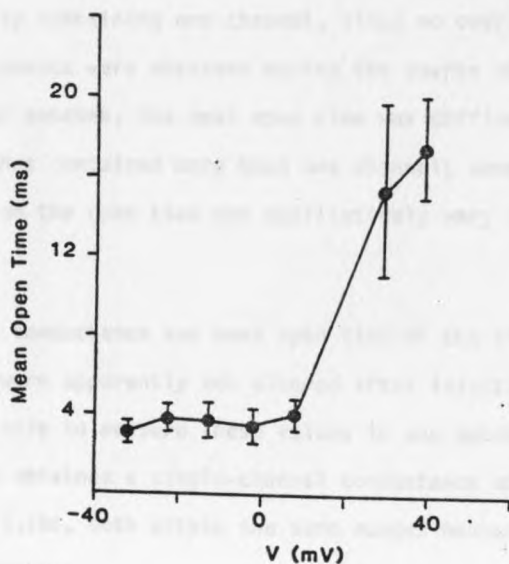
**FIGURE 9.** Voltage-dependence of the light-activated channel mean open time. a. Patch current recordings obtained at various patch potentials. The numbers at the left indicate absolute patch potentials (intracellular potential minus pipette potential). Filter:  $\tau = 0.8\text{ms}$ . b. Plot of the mean open time vs. voltage of data from the same patch as in A. The mean open times were calculated as the average open time  $\pm$  S.D. No overlapping of single-channel currents was observed for this patch, suggesting that the patch contained a single light-activated channel. The patch did not contain voltage-dependent channels.



a

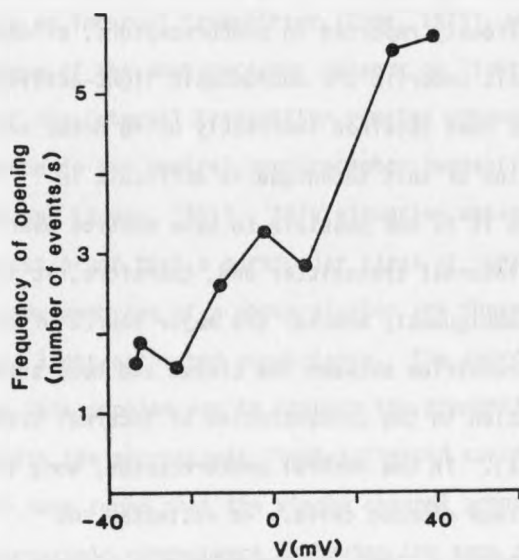


b



Frequency of opening of the channel vs. potential. The probability of opening of the light-activated channel can also be measured in the same patch as in Fig. 9. The frequency of channel opening during the maintained response to a steady light is plotted as a function of potential in Fig. 10. The plot shows that the frequency of opening of the channel increases ~4-fold with an 80mV increase in the patch potential. This effect was observed consistently in the patches in which this was examined (4), but only in this patch were we able to quantify the results. The other patches contained several light-activated channels.

**FIGURE 10.** Voltage-dependence of the frequency of opening of the light-activated channel. The plot shows the frequency of opening (number of events/s) vs. voltage, and was obtained by counting the number of channel openings in each period of time at various absolute patch potentials (intracellular potential minus the pipette potential). The data was taken from the same patch as in Fig. 9, which contained one light-activated channel and no voltage-dependent channels.



## DISCUSSION

In this Chapter we report that the ventral photoreceptor membrane contains ionic channels which are activated by light. Furthermore, we present evidence indicating that such channels underlie the macroscopic light-activated conductance.

### Previous Evidence for Channels in Photoreceptors.

Although no direct observation of light-activated single-channel currents has been previously reported in photoreceptors, evidence suggesting that channels underlie the macroscopic light-activated conductance change has been obtained indirectly using noise analysis. However, the application of this technique is difficult in photoreceptors because it is not possible to have control over the concentration of the internal transmitter and, therefore, it is not possible to decide unambiguously whether the major source of the fluctuations is the transition between the closed and open states of the channels or the variation in the concentration of internal transmitter (Fain and Lisman, 1981). In the ventral photoreceptor, Wong (1978) used this technique on voltage clamped cells. He estimated the single-channel conductance as 18pS and the mean open time as 18.7ms. These values, considering the assumptions involved in their determination, are rather close to those measured by us in the same cells.

Recently, analysis of patch current fluctuations in vertebrate rods suggested a unitary conductance of 50fS for the light-dependent conductance, a value compatible with a channel of unusually small

conductance or with a carrier (Detwiler et al, 1982). Studies of the voltage noise of photoreceptors have also been done (Lamb and Simon, 1977; Schwarz, 1977; Payne, 1981). However, these studies have the additional complication of the possible contribution of voltage-dependent channels to the noise.

#### Evidence for the Light-activation of the Channels.

The activation of the light-activated channels is thought to be mediated by an internal transmitter (Cone, 1973), whose concentration in the cytoplasm of the photoreceptor depends on light intensity. The identity of the internal transmitter remains unknown, although there is good evidence in the ventral photoreceptor suggesting that it cannot be  $\text{Ca}^{2+}$  (Fain and Lisman, 1981). This situation makes it very difficult to obtain direct proof that a particular class of ionic channels detected in the plasma membrane of a photoreceptor are those underlying the macroscopic light-activated conductance. The approach that we undertook to address this problem was to compare the properties of the single channels with the macroscopic light-activated current (Fain and Lisman, 1981). We have found that the single channel properties resemble those of the macroscopic conductance in having the same reversal potential, in that their light-activation is not mediated by voltage or by  $\text{Ca}^{2+}$ , in having qualitatively similar intensity- and time-dependence of activation and finally in having qualitatively similar properties of light-adaptation. They differ in the latency of activation and in the absolute light-intensity necessary to induce their activation. Below we discuss the similarities and differences between the single-channel conductance and the macroscopic light-activated conductance.

Similarities Between the Single Channels and the Macroscopic  
Light-activated Conductance.

Reversal potential. We found that the reversal potential ( $\sim +9\text{mV}$ ) of the channels activated by light is in the same range as that of the macroscopic light-activated current (Millecchia and Mauro, 1969c).

The macroscopic light-activated conductance has been previously shown to be voltage-dependent (Millecchia and Mauro, 1969c), becoming larger at positive potentials. This could be due to voltage-dependence of the single-channel conductance, its mean open time, its probability of opening, or to a combination of these factors. We found that the single-channel conductance is independent of voltage within the same potential range used in the macroscopic studies (Fig. 7b). However, the mean open time and the probability of opening during light were found to increase at positive voltages (Figs. 9 and 10). This voltage-dependence of the mean open time and probability of opening can qualitatively account for the voltage-dependence of the macroscopic conductance. The increase in the probability of opening of the channel may reflect an effect of voltage directly on the channel or an effect of voltage on the mechanisms for release or uptake of the internal transmitter. From our data we cannot decide between these possibilities.

Voltage does not induce activation of the channels. The macroscopic light-activated conductance is not activated by depolarizing the photoreceptor membrane in the dark (Fain and Lisman, 1981). Similarly, the light-activated channels cannot be opened by depolarizing the cell in the dark.

Ca<sup>2+</sup> does not induce activation of the channels. Internal free Ca<sup>2+</sup> rises during light (Fain and Lisman, 1981) and produces a reduction in the light-activated current (light-adaptation). Injection of EGTA into the photoreceptor, which abolishes the rise in intracellular Ca<sup>2+</sup>, increases the maintained phase of the macroscopic light-activated current. In our experiments, injection of EGTA produced an enhancement of the light-induced single-channel activity (Fig. 6), in agreement with the macroscopic data. If the channel were a Ca<sup>2+</sup>-activated channel, the activity should have been depressed by the EGTA-injection. Therefore, we ruled out the possibility of a Ca<sup>2+</sup>-activated channel.

Intensity and time-dependence. The activation of the macroscopic light-activated conductance is graded with light intensity. We found that the activation of the single-channels is also graded with light intensity in a qualitatively similar way (Fig.4).

The macroscopic light-activated current evoked by a prolonged dim light in a voltage-clamped ventral photoreceptor has been shown previously to consist of a steady inward current, whereas bright lights produce inward currents consisting of an early transient which declines to a lower, steady-state level (Millecchia and Mauro, 1969c). We found that in all patches the light-activation of the channels followed a qualitatively similar time-course as the macroscopic current to bright lights: the single-channel activation had an initial transient phase of high probability of channel opening which was followed by a phase of lower and maintained rate of channel opening until the termination of the light (Fig. 4). In one of these patches we observed, in addition, a single, steady phase of channel activity at dimmer light (see Fig. 3),



resembling the waveform of the macroscopic current evoked by a dim light.

Light-adaptation and the effect of EGTA. An adapting light transiently decreases the macroscopic current evoked by a test flash (Lisman and Brown, 1971b). We have found that the single-channel response adapts to light in a qualitatively similar way (Fig. 5). The single-channel response was depressed after an adapting light, but it recovered after the cell had dark-adapted.

Differences Between the Single-channels and the Macroscopic Light-activated Conductance.

Latency. The latency of the single-channel responses was in all cases longer than in the corresponding macroscopic responses. The reason for this long latency could be that in our experiments we may have preferentially recorded from membrane patches with an unusual spatial relationship with the rest of the transduction machinery, thus presenting a behavior somewhat shifted from the average. This could be a normal situation in the cell or, alternatively, it could result from the procedures required to obtain seals. The regions of the cell membrane suitable for seal formation may have been altered by the sonication. Alternatively, alteration of the membrane morphology produced by the patch electrode itself may be critical; the patch membrane folds into the pipette, presenting an  $\Omega$ -shape (Hamill et al, 1981) and leaving a narrow path connecting the cytoplasm with the patch membrane. If the probability of opening of a light-dependent channel depends on the diffusion of internal transmitter through this distorted path, the change in transmitter concentration in the patch might be slow

compared to the channels of rest of the membrane. This would result in a shift in the kinetics of activation of the patch channels relative to the activation of the macroscopic current.

Intensity of activating light. The activation of the channels was induced in all patches with lights much brighter (by 3 log units or more) than those needed to produce a detectable macroscopic response. The reason for this shift in the activation threshold can be explained by the same argument used to explain the latency. The change in concentration of transmitter at the patch channel would vary much less and more slowly than the change in transmitter concentration near the 'average' channel, such that a relatively brighter light was necessary to trigger activation of the single channels at the patch compared to that necessary to activate the macroscopic conductance.

Altogether, the evidence presented in this paper strongly suggests that the single-channels that we have studied are activated by light and underlie the macroscopic light-activated conductance in the ventral photoreceptor.

Possible Effect of  $\text{Ca}^{2+}$  on the Light-activated Channel.

The light-induced rise in intracellular free  $\text{Ca}^{2+}$  concentration has a role in light-adaptation: it reduces the light-activated conductance in ventral photoreceptors (Lisman and Brown, 1975). However, the mechanism by which  $\text{Ca}^{2+}$  produces this effect remains unknown. One possibility is that it acts directly on the channel; alternatively, it may have an effect on the release of transmitter (either directly or on some previous step leading to it) or on the mechanism of uptake of

transmitter. From our data, we cannot distinguish between these possibilities, which are in no way exclusive. However, our results put some constraint on the kind of direct interaction that  $\text{Ca}^{2+}$  could have with the channel. The action of  $\text{Ca}^{2+}$  on the channel could be to decrease its conductance, to decrease its mean open time or decrease its probability of opening. In our experiments there was no obvious change in the single-channel conductance or mean open time at the various light intensities that we used to stimulate the cells (-3.0 to 0). Since the levels of  $\text{Ca}^{2+}$  concentration are expected to vary at these different intensities (Levy, 1983),  $\text{Ca}^{2+}$  does not appear to have an important effect on these properties of the channel under our experimental conditions.  $\text{Ca}^{2+}$  could, however, decrease the probability that the channel opens by blocking the channel gate. This blockade would have to occur when the channel is in the closed state and not when it is open, because otherwise we should see a change in the mean open time, which was not observed. In conclusion, the only type of direct effect of  $\text{Ca}^{2+}$  on the channel not excluded by our data is a blockade of the gate of the gate when the channel is closed.

#### Comparison of the Properties of the Light-activated Channel and the Acetylcholine Channel.

The single light-activated channels in Limulus appear to be "classic" channels and are remarkably similar to the acetylcholine-activated channel. Both channels are controlled by a transmitter, although the unknown molecule that controls the light-activated channel acts from the inside of the photoreceptor membrane, whereas acetylcholine binds to the acetylcholine

receptor-channel complex from the external side. Their single-channel conductance and mean open time are similar. Using similar conditions of temperature and ionic strength as ours, Montal et al (1984) measured a single-channel conductance of 48pS and a mean open time in the millisecond range for the acetylcholine receptor from Torpedo electric organ reconstituted in phospholipid bilayers. These values are very close to those measured by us for the light-activated channel (45 pS and 4mS, respectively). The selectivity properties of both channels are also very similar: the reversal potentials of the currents flowing through both channels is near zero (see above and Adams et al, 1980) and the permeability ratio for various cations is also quite similar for both channels (Brown and Mote, 1974; Adams et al, 1980; Montal et al, 1984).

The reversal potential of the light-activated current (0 to +20mV; Millecchia and Mauro, 1969c ; Brown and Mote, 1974), is somewhere in between the reversal potential for  $\text{Na}^+$  and for  $\text{K}^+$ , which are the principal ions that carry current across the ventral photoreceptor membrane (Fain and Lisman, 1981). The net inward current flowing through the light-activated conductance is carried principally by  $\text{Na}^+$ . The permeability ratio for  $\text{Na}^+/\text{K}^+ = \sim 2$  (Brown and Mote, 1974). One possible explanation for a macroscopic conductance having such a selectivity ratio for these cations is that it consists of two different channels: a  $\text{Na}^+$ -selective channel and a  $\text{K}^+$ -selective channel, both of which would be simultaneously opened by light. A model such as this was proposed by Takeuchi and Takeuchi (1960) for the acetylcholine-activated conductance in the neuromuscular junction which, as mentioned above, has a similar ionic selectivity as the light-activated conductance. This

possibility has been ruled out for the neuromuscular junction (Adams et al, 1980) and is now ruled out for Limulus light-activated conductance by our single-channel data. The light-activated single-channel currents that have the same reversal potential as the macroscopic light-activated current, whereas if the two-channel theory were correct, we should have found two different channels, one having a much more positive reversal potential (a  $\text{Na}^+$ -channel) and another with a more negative reversal potential (a  $\text{K}^+$ -channel).

#### Implications of the Single-channel Basis for the Light-activated Conductance with Regard to Transduction.

One remarkable characteristic of light-transduction is the gain involved in this process. With the mean open time and the single-channel current at a certain potential, we can calculate the number of channel openings that occur during an average quantum bump in a dark-adapted ventral photoreceptor. In a cell voltage-clamped to resting potential, the quantum bump current is typically  $\sim 2\text{nA}$  at the peak and has a duration of  $\sim 100\text{ms}$ . The charge mobilized during such a bump is  $6 \times 10^8$  electronic charges (Goldring, 1983). The charge mobilized when a light-activated channel opens for  $4\text{ms}$  (approximate value of the mean open time of the channel) in a patch at resting potential is  $2.4 \times 10^4$  electronic charges. Therefore, approximately  $10^4$  channel openings occur during the average quantum bump. This means that for each rhodopsin molecule isomerized by light,  $10^4$  channel openings are induced, which is the gain of the process at low light intensities. A value of  $10^3$  channel openings/bump was estimated by Wong (1978), based on noise analysis determinations of the channel conductance and mean open time

(see below). The quantum bump current relaxes with a time constant of 14.4ms (Wong, 1978). Because the mean open time of the light-activated channel is much shorter than that, the relaxation of the bump cannot be determined by the time constant of closing of the channels but rather it reflects the change in the concentration of internal transmitter. This situation is different than in the miniature end plate potentials of the postsynaptic membrane of the neuromuscular junction; in such a case, the relaxation is determined by the closing of the acetylcholine-activated channels (Anderson and Stevens, 1973).

## REFERENCES

- Adams, D.J., Dwyer, T.M. and Hille, B. 1980. The permeability of endplate channels to monovalent and divalent metal cations. *J. Gen. Physiol.* 75: 493-510.
- Anderson, C.R. and Stevens, C.F. 1973. Voltage clamp analysis of acetylcholine produced end-plate current fluctuations at frog neuromuscular junction. *J. Physiol.* 235: 655-691.
- Bacigalupo, J., J. Stern and J. Lisman. 1981. Structural and functional specialization of Limulus ventral photoreceptor membrane. *Invest. Ophthalm. Mol. Visual Sci.* 20: 181.
- Baylor, D.A., Lamb, T.D. and Yau, K-W. 1979. The membrane current of single rod outer segments. *J. Physiol.* 228: 589-611.
- Brown, J.E. and Blinks, J.R. 1974. Changes in intracellular free calcium concentration during illumination of invertebrate photoreceptors: detection with aequorin. *J. Gen. Physiol.* 64: 643-665.
- Brown, J.E. and Mote, M.I. 1974. Ionic dependence of reversal voltage of the light response in Limulus ventral photoreceptors. *J. Gen. Physiol.* 63: 337-350.
- Brown, J.E., Brown, P.K. and Pinto, L.H. 1977. Detection of light-induced changes of intracellular ionized calcium concentration in Limulus ventral photoreceptors using Arsenazo III. *J. Physiol.* 267: 299-320.
- Brown, J.E., H.H. Harary and A. Waggoner. 1979. Isopotentiality and an optical determination of series resistance in Limulus ventral photoreceptors. *J. Physiol.* 296: 357-372.
- Baylor, D.A., Matthews, G. and Yau, K-W. 1980. Two components of electrical dark noise in toad retinal rod outer segments. *J. Physiol.* 309: 591-621.
- Calman, B. and Chamberlain, S. 1982. Distinct lobes of Limulus ventral photoreceptors. II Structure and ultrastructure. *J. gen. physiol.* 80: 839-862.
- Chinn, K.S. and Lisman, J.E. Calcium mediates the light-induced decrease in maintained outward current in Limulus ventral photoreceptors. Submitted for publication.

- Clark, A.W., Millecchia, R. and Mauro, A. 1969a. The ventral photoreceptor cells of Limulus. I. The microanatomy. J. Gen Physiol. 54:289-309.
- Cone, R.A. 1973. The internal transmitter model for visual excitation: some quantitative implications. In Biochemistry and Physiology of Visual Pigments (Ed. H. Langer), p. 275. Springer-Verlag, Berlin.
- Conti, F., DeFelice, L.J. and Wanke, E. 1975. Potassium and sodium ion current noise in the membrane of the squid giant axon. J. Physiol. 262: 699-727.
- DeFelice, L.J. and Alkon, D.L. 1977. Voltage noise from hair cells during mechanical stimulation. Nature 269: 613-615.
- Detwiler, P.B., Conner, J.D. and Bodoia, R.D. 1982. Gigaseal patch clamp recordings from outer segments of intact retinal rods. Nature 300: 59-61.
- Dodge, F.A., Knight, B.W. and Toyoda, 1968. Voltage noise in Limulus visual cells. Science 160: 88-90.
- Fain, G.L. and Lisman, J.E. 1981. Membrane conductances of Photoreceptors. Prog. Biophys. molec. Biol. 37: 91-147.
- Fein, A. and J.S. Charlton. 1975. Local membrane current in Limulus photoreceptors. Nature 258: 250-252.
- Fein, A. and J.E. Lisman. 1975 Localized desensitization of Limulus photoreceptors produced by light or intracellular calcium ion injection. Science 187: 1094-1096.
- Fein, A. and Szuts, E.Z. 1982. Photoreceptors: their role in vision. Cambridge University Press.
- Fuortes, M.G.F. and Hodgkin, A.L. 1964. Changes in time scale and sensitivity in the ommatidia of Limulus. J. Physiol. 172: 239-263.
- Fuortes, M.G.F. and S. Yeandle. 1964. Probability of Occurrence of Discrete Potential Waves in the Eye of Limulus. J. Gen. Physiol. 47: 443-463.
- Goldring, M. 1982. Ph.D. Thesis. Brandeis University.
- Goldsmith, T.H., Dizon, A.E. and Fernandez, H.R. 1968. Microspectrophotometry of photoreceptor organelles from eyes of the prawn Palaemonetes. Science 161: 468-470.
- Hamill, O.F., Marty, A., Neher, E., Sackmann, B. and Sigworth, F.S. 1981. Improved patch-clamp techniques for high-resolution current recording from cells and cell-free membrane patches. Pfluegers Arch. 391: 85-100.



- Harary, H.H. and J.E. Brown. 1981. Rapid-Scanning Photometric Examination of intracellular Arsenazo III in Limulus Ventral Photoreceptors. Biophysics J. 33: 205a.
- Lamb, T.D. and Simon, E.J. 1977. Analysis of electrical noise in turtle cones. J. Physiol. 272: 435-468.
- Langer, H. and Thorell, B. 1966. Microspectrophotometry of single rhabdomeres in the insect eye. Exp. Cell Res. 41: 673-677.
- Latorre, R., Coronado, C. and Vergara, C. Channels gated by voltage and ions. Annual Rev. of Physiol. In Press.
- Leonard, R.J. and Lisman, J.E. 1981. Light modulates voltage-dependent potassium channels in Limulus ventral photoreceptors. Science 212: 1273-1275.
- Levy, S. 1983. Ph.D. Thesis. Boston University.
- Lisman, J.E. and Brown, J.E. 1971a. Two light-induced processes in the photoreceptor cells of Limulus ventral eye. J. Gen Physiol. 58: 544-561.
- Lisman, J.E. and Brown, J.E. The effects of intracellular  $Ca^{2+}$  on the light response and on light adaptation in Limulus ventral photoreceptors. 1971b. In The Visual System: Neurophysiology, Biophysics and their clinical applications. (Ed. G.B. Arden), p. 23-33. Plenum Publisher, N.Y.
- Lisman, J.E. and J.E. Brown. 1972. The effect of iontophoretic injection of calcium and sodium ions on the light response of Limulus ventral photoreceptors. J. Gen. Physiol. 59: 701-719.
- Lisman, J.E. and Brown, J.E. 1975. Effects of intracellular injection of calcium buffers on light adaptation in Limulus ventral photoreceptors. J. Gen. Physiol. 66: 489-506.
- Lisman, J.E., Fain, G.L. and O'Day, P.M. 1982. Voltage-dependent conductances in Limulus ventral photoreceptors. J. Gen Physiol. 79: 187-209.
- Millecchia, R. and Mauro, A. 1969b. The ventral photoreceptor cells of Limulus. II. The basic photoresponse. J. Gen Physiol. 54: 310-330.
- Millecchia, R. and Mauro, A. 1969c. The ventral photoreceptor cells of Limulus. III. A voltage clamp study. J. Gen. Physiol. 54: 331-351.
- Payne, R. Suppression of noise in a photoreceptor by oxidative metabolism. 1981. J. Comp. Physiol. 142: 181-188.
- Montal, M., Labarca, P., Fredkin, D.R., Suarez-Isla, B.A. and Lindstrom, J. Channel properties of the purified acetylcholine receptors from Torpedo californica reconstituted in planar lipid bilayers. In Press.

- Muruyama, Y. and Petersen, OhH. Single-channel currents in isolated patches of plasma membrane from basal surface of pancreatic acini. 1982. Nature 299: 159-161.
- Neher, E. and Sackmann, B. 1976. Single-channel currents recorded from membrane of denervated muscle fibres. Nature 260: 799-802.
- Payne, R. 1981. Suppression of noise in a photoreceptor by oxidative metabolism. J. Comp. Physiol. 142: 181-188.
- Schwartz, E.A. 1977. Voltage noise observed in rods of the turtle retina. J. Physiol. 272: 217-246.
- Stern, J. Chinn, K., Bacigalupo, J. and Lisman, J.E. Distinct lobes of Limulus ventral photoreceptors. I. Functional and anatomical properties of lobes revealed by removal of glial cells.
- Takeuchi, A and Takeuchi, N. 1960. On the permeability of the end-plate membrane during the action of transmitter. J. Physiol. 154: 52-67.
- Wong, F. 1978. Nature of light-induced conductance changes in ventral photoreceptors of Limulus. Nature 276: 76-79.
- Wong, F., R.B. Leonard, N.E. Kremer and R.M. Denney. 1982. Invest. Ophthalmol. Visual Sci. 22: 205.
- Yeandle, S. 1958. Evidence of quantized slow potentials in the eye of Limulus. Am. J. Ophthalmol. 46: 82-87.
- Yellen, G. 1982. Single  $\text{Ca}^{2+}$ -activated nonselective cation channels in neuroblastoma. Nature 296: 357-359 (1982).

